International Geology Review

ISSN: 0020-6814 (Print) 1938-2839 (Online) Journal homepage: http://www.tandfonline.com/loi/tigr20

The Proterozoic evolution of northern Siberian Craton margin: a comparison of U–Pb–Hf signatures from sedimentary units of the Taimyr orogenic belt and the Siberian platform

Nadezhda Priyatkina, William J. Collins, Andrei Khudoley, Dmitry Zastrozhnov, Victoria Ershova, Kevin Chamberlain, Andrey Shatsillo & Vasily Proskurnin

To cite this article: Nadezhda Priyatkina, William J. Collins, Andrei Khudoley, Dmitry Zastrozhnov, Victoria Ershova, Kevin Chamberlain, Andrey Shatsillo & Vasily Proskurnin (2017) The Proterozoic evolution of northern Siberian Craton margin: a comparison of U–Pb–Hf signatures from sedimentary units of the Taimyr orogenic belt and the Siberian platform, International Geology Review, 59:13, 1632-1656, DOI: 10.1080/00206814.2017.1289341

To link to this article: http://dx.doi.org/10.1080/00206814.2017.1289341

INTERNATIONAL GEOLOGY REVIEW, 2017
VOL. 59, NO. 13, 1632–1656
https://doi.org/10.1080/00206814.2017.1289341

Taylor & Francis
Taylor & Francis Group

The Proterozoic evolution of northern Siberian Craton margin: a comparison of U–Pb–Hf signatures from sedimentary units of the Taimyr orogenic belt and the Siberian platform

Nadezhda Priyatkina[a], William J. Collins[a,b], Andrei Khudoley[c], Dmitry Zastrozhnov[d,e], Victoria Ershova[c], Kevin Chamberlain[f,g], Andrey Shatsillo[h] and Vasily Proskurnin[d]

[a]New South Wales Institute of Frontiers Geoscience, University of Newcastle, Newcastle, NSW, Australia; [b]Department of Applied Geology, Curtin University, Perth, WA, Australia; [c]Institute of the Earth Sciences, St. Petersburg State University, St. Petersburg, Russia; [d]All Russian Geological Research Institute (VSEGEI), St. Petersburg, Russia; [e]Centre for Earth Evolution and Dynamics (CEED), University of Oslo, Oslo, Norway; [f]Department of Geology and Geophysics, University of Wyoming, Laramie, WY, USA; [g]Faculty of Geology and Geography, Tomsk State University, Tomsk, Russia; [h]Laboratory of Main Magnetic Field and Paleomagnetism, Institute of the Earth Physics (IFZ RAN), Moscow, Russia

ABSTRACT
Identifying the cratonic affinity of Neoproterozoic crust that surrounds the northern margin of the Siberian Craton (SC) is critical for determining its tectonic evolution and placing the Craton in Neoproterozoic supercontinental reconstructions. Integration of new U–Pb–Hf detrital zircon data with regional geological constraints indicates that distinct Neoproterozoic arc-related magmatic belts can be identified within the Taimyr orogen. Sedimentary rocks derived from 970 to 800 Ma arc-related suites reveal abundant Archean and Paleoproterozoic detritus, characteristic of the SC. The 720–600 Ma arc-related zircon population from the younger Cambrian sedimentary rocks is also complemented by an exotic juvenile Mesoproterozoic zircon population and erosional products of older arc-related suites. Nonetheless, numerous evidences imply that both arcs broadly reworked Siberian basement components. We suggest that the early Neoproterozoic (ca. 970–800 Ma) arc system of the Taimyr orogen evolved on the active margin of the SC and probably extended along the periphery of Rodinia into Valhalla orogen of NE Laurentia. We also suggest the late Neoproterozoic (750–550 Ma) arc system could have been part of the Timanian orogen, which linked Siberia and Baltica at the Precambrian/Phanerozoic transition.

ARTICLE HISTORY
Received 25 November 2016
Accepted 28 January 2017

KEYWORDS
Siberia; U–Pb–Hf isotopes; detrital zircon; Arctic; Proterozoic

1. Introduction

Neoproterozoic orogenic belts in the Arctic region are some of the least studied of Earth's crustal domains, largely because of their poor accessibility. One of them is the Taimyr orogen, which extends across the northern margin of the Siberian Craton (SC, Figure 1(a)). The Taimyr orogen is divided into three structural domains (Zonenshain *et al*. 1990; Uflyand *et al*. 1991; Vernikovsky 1996). The northern domain is a part of the Kara terrane, comprising uppermost Neoproterozoic to Lower Cambrian deformed turbidite succession (Uflyand *et al*. 1991; Vernikovsky 1996). The southern domain comprises uppermost Ediacaran–Triassic carbonate rocks and siliciclastics of the SC margin. The third central domain is the Neoproterozoic Central Taimyr Belt (CTB), which partly underlies the southern domain (Figure 1(b)).

The CTB incorporates supra-subduction suites and ophiolitic rocks dated between 970 and 600 Ma (Figure 1(b), e.g. (Vernikovsky 1996; Pease and Vernikovsky 2000; Vernikovsky and Vernikovskaya 2001; Vernikovsky *et al*. 2004; Kachurina *et al*. 2012; Proskurnin *et al*. 2014), indicating that it was part of a subduction–accretion complex during the Neoproterozoic. However, it remains ambiguous whether the CTB formed on the active margin of northern SC or was exotic.

Geological and palaeomagnetic records concerning Neoproterozoic terrane affinity in the CTB are scarce. The northern domain is separated from the CTB by a late Paleozoic thrust (Uflyand *et al*. 1991; Vernikovsky 1996). At the southern margin of the CTB (Figure 1(b)), a major unconformity (Uflyand *et al*. 1991; Vernikovsky 1996; Vernikovsky *et al*. 2004), defined by an onlap assemblage of latest Neoproterozoic and Paleozoic

CONTACT Nadezhda Priyatkina nadezda.priyatkina@uon.edu.au New South Wales Institute of Frontiers Geoscience, University of Newcastle, Newcastle, NSW 2308, Australia
Supplemental data for this article can be accessed here

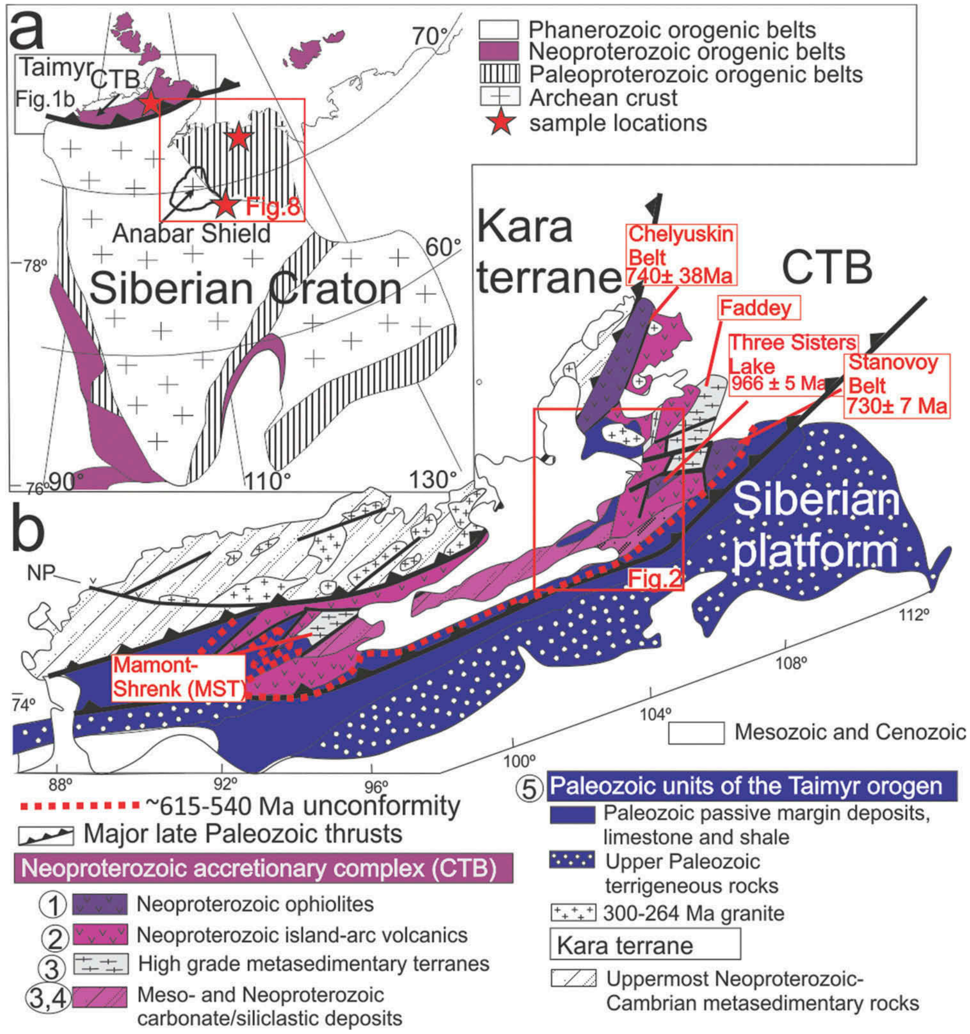

Figure 1. Location of samples on the schematic maps of Siberian Craton (a) and the Taimyr orogen (b). Archean and Paleoproterozoic crustal units of Siberian Craton simplified after Rosen (2003). Schematic map (b) showing the relationship between main geological units of the Taimyr orogenic belt after Vernikovsky and Vernikovskaya (2001). Numbers against the Central Taimyr Belt (CTB) units are references in text of Section 2.1.

sediments, indicates that the southern and central domains were juxtaposed during the Ediacaran, but there is no evidence for any pre-Ediacaran relationship.

An unusual Grenville-related metasedimentary fragment within the Taimyr belt, called the Mamont-Shrenk terrane (Pease *et al*. 2001), further referred to as MST, suggests an exotic origin at least for some of the CTB terranes. This is consistent with some palaeomagnetic interpretations (Proskurnin *et al*. 2014) suggesting that an 870–820 Ma continental arc-related I-type granitoid belt in the CTB formed nearly 3000 km to the north of the SC. By contrast, similar palaeomagnetic analysis for earlier 970 Ma oceanic arc terranes of the CTB suggests it was only separated from the SC by a back-arc basin (Vernikovsky *et al*. 2011), implying a peri-Siberian origin. Until this controversy is resolved, the evolution of CTB and the northern margin of the SC cannot be established.

Establishment of terrane affinities to original cratonic margins is commonly assessed using a U–Pb–Hf in zircon approach (Kuznetsov *et al*. 2010; Abati *et al*. 2012; Linnemann *et al*. 2014; Henderson *et al*. 2016). However, limited detrital zircon studies (e.g. Kachurina *et al*. 2012) have been reported from Proterozoic successions of the Taimyr orogenic belt, and only few studies (Khudoley *et al*. 2015; Kuptsova *et al*. 2015; Priyatkina *et al*. 2016) have presented U–Pb detrital zircon datasets from the northern part of the SC. In attempt to characterize the Neoproterozoic crust within the CTB and identify its original cratonic affinity, we first present U–Pb–Hf detrital zircon signatures from pre-orogenic (Mesoproterozoic), syn-orogenic

(Neoproterozoic) and post-orogenic (early Cambrian) successions of the CTB (Figure 1(a,b)). They are compared and contrasted with coeval sedimentary records on the platform to evaluate the provenance relationship to Archean and Paleoproterozoic units of the SC.

2. Overview of the analytical procedures

Full description of analytical procedures used in this study is presented in Supplementary file 1. U–Pb–Hf detrital zircon analyses were guided by CL and transmitted light imaging. The majority of detrital zircon data used here were laser ablation inductively coupled plasma mass spectrometry (LA-ICP-MS) U–Pb analyses carried out at the University of Newcastle (Australia). These data are presented in Supplementary material 2. Additional U–Pb analyses of the zircons were performed using SHRIMP-II ion microprobe (Center of Isotopic Research, VSEGEI, St. Petersburg, Russia). SHRIMP data are presented separately in Supplementary file 3. Concordia plots for each sample are presented in Supplementary file 4. For constructing age, probability distribution plots and further interpretation analyses with discordance greater than 10% were filtered, as well as grains with 2σ error higher than 10%. For the analysed samples we commonly present two values of maximum depositional age (MDA), calculated using two different methods suggested by (Dickinson and Gehrels 2009). These include (1) youngest single grain (YSG) age, and (2) a more conservative estimate based on mean age of the youngest cluster ($n \geq 3$) of grain ages that overlap in age at 2σ, further referred to as mean age of the youngest cluster.

Dating of mafic sills was performed by *in situ* SIMS U–Pb baddeleyite dating technique (data in Supplementary file 5). Hf in zircon analyses were carried out in advanced Analytical Centre at James Cook University, Townsville (Australia) using a GeoLas 193-nm ArF laser and a Thermo Scientific Neptune multi-collector ICP-MS.In the data tables, Hf in zircon data are linked to each U–Pb single grain analysis (Supplementary files 2 and 3).

3. CTB

The CTB is a collage of dominantly Meso- to-late Neoproterozoic terranes that were accreted to the northern margin of the SC before erosion and deposition associated with the regional Ediacaran unconformity (Figure 1(b)). Post-unconformity units represent an onlap assemblage originally connected to the northern passive margin of the SC, but they were subsequently folded and thrusted during Carboniferous-Permian orogeny, when the Kara terrane collided to the SC (Pease 2011; Metelkin *et al*. 2012; Vernikovsky *et al*. 2013). Major units of the CTB include: (1) ophiolites, (2) arc volcanics and granites, (3) metasedimentary basement terranes, (4) late Neoproterozoic pre-unconformity metasedimentary units, and (5) Ediacaran and Paleozoic post-unconformity sedimentary rocks of the SC passive margin.

3.1. Main tectonics units of the CTB

(1) *Ophiolites and associated rock units*. The Chelyuskin and Stanovoy ophiolitic fragments ((1) in Figure 1(b)) are represented by north-easterly trending slices of serpentinized ultramafics, gabbroic rocks, locally overlain by deep marine sedimentary rocks (Vernikovsky 1996). In both the ophiolitic belts, up to ~2.5 km thick units of metaperidotite and metagabbro coexist in a thrust contact with tholeiitic to calc-alkaline rock association, within which silica contents are variable (Vernikovsky *et al*. 1994, 1996; Vernikovsky 1996). In the Chelyuskin belt, a plagiogranite, a metarhyolite, and a metagabbro of the Kunar-Mod igneous rock association yield U–Pb zircon ages of 755 ± 7 Ma (Vernikovsky *et al*. 2004), ~ca. 630 and 615 ± 12 Ma (Pease and Vernikovsky 2000), respectively. Similar plagiogranites occur in Stanovoy, but the only U–Pb zircon age has been obtained for Zimovnichaya gabbro, which emplacement (730 ± 7 Ma, Vernikovsky *et al*. 2004) was nearly coeval with early Kunar-Mod volcanics. Late Neoproterozoic metamorphic rocks have been reported from fringes of the Stanovoy belt (Vernikovsky and Zabiyaka 1985; Makhlaev 1988; Vernikovsky 1995, 1996), including garnet amphibolite (~590–630 Ma, K–Ar, Vernikovsky *et al*. 1997) and kyanite-bearing schist formed at 600–650°C and 5.5–8.5 kbar, as well as fragmentary eclogites.

(2) *Other arc-related magmatic belts*. The oldest arc-related suite in the CTB is represented by the Three Sisters Lake terrane ((2) in Figure 1(b)). It incorporates mafic, intermediate and felsic rock association, including a plagiogranite and its volcanic analogue dated at 967 ± 17 and 966 ± 5 Ma, respectively (U–Pb, zircon, Vernikovsky *et al*. 2011). Geochemically similar to volcanic rocks associated with Stanovoy and Chelyuskin Belts, the rocks have been referred to as an island arc fragment (Vernikovsky *et al*. 2011). Same as much more widespread early Neoproterozoic S- and I-type granites, best exemplified by the 870–820 Ma Zhdanov and the Snezhinsky granite suites (Vernikovsky *et al*. 1998; Pease and

Vernikovsky 2000; Kuz'min *et al*. 2007; Proskurnin *et al*. 2014), the Three Sisters Lake magmatic arc complex was emplaced into the Oktyabr'–Zhdanov succession (Vernikovsky *et al*. 2011). In the MST (Figure 1(b)), reported ages of granitoids are older, e.g. ca. 900–885, 940–920 Ma (Pease *et al*. 2001). Younger magmatic arc suites include ca. 630 Ma two-mica granite of the Faddey terrane (Pease and Vernikovsky 2000).

(3) *Mesoproterozoic to earliest Neoproterozoic basement metasedimentary terranes*. Metasedimentary basement terranes of the CTB are traditionally subdivided into two types based on their metamorphic grade (Vernikovsky 1996), namely the low-grade and the high-grade (Figure 1(b)). The low-grade terrane is entirely represented by silisiclastic and carbonate metasedimentary deposits of the Oktyabr'–Zhdanov Group, the host unit for Severobyrrang mafic complex (Proskurnin *et al*. 2009), which new baddelyite U–Pb age is discussed later. High-grade metasedimentary terranes of early Neoproterozoic age are exemplified by the Mamont-Shrenk and Faddey basement units ((3) in Figure 1(b)). These are dominated by mature, amphibolite facies metapelitic units, including cordierite-bearing, biotite-sillimanite, and garnet-biotite schists (Vernikovsky 1996), yielding maximum depositional zircon age of 1004 ± 17 Ma (Mamont-Shrenk terrane only, Pease *et al*. 2001). They metasedimentary successions were metamorphosed under temperatures of ~500–650°C and pressures of ~5.5–8.0 kbar (Vernikovsky and Zabiyaka 1985; Vernikovsky 1995). In the MST and Faddey terrane, late Neoproterozoic metamorphism has lead to zircon growth and resetting of the U–Pb isotopic system at 700–600 Ma. The younger age limits of both low- and high-grade metasedimentary terranes are defined by early Neoproterozoic crosscutting granitoids (2).

(4) *Neoproterozoic metasedimentary formations ((4) in Figure 1(b))*. These formations unconformably overlie, or are in faulted contact with the abovementioned Mesoproterozoic to earliest Neoproterozoic metasedimentary basement terranes, or non-conformably overlie the Early Neoproterozoic magmatic suites. The most important units include molasse-type Stanovskaya Formation and the Kolosovo Formation, a dismembered carbonate platform (Vernikovsky 1996).

(5) *Post ~615–540 Ma unconformity sedimentary succession*. Unconformably overlying the basement ((1)–(4) in Figure 1(b)), the succession ((5) in Figure 1 (b)) forms transgressive sedimentary cycle, commencing with a 20 m thick post-orogenic siliciclastic succession, a part of Nizhneostantsovaya Formation. Siliciclastic rocks pass into limestone and shale sequence of the Paleozoic SC passive margin.

3.2. Stratigraphic setting and description of the studied sedimentary units

The studied samples from the CTB are located in Meso- to Neoproterozoic sedimentary successions adjacent to the Faddey metamorphic terrane (Figure 1(b), see also Figure 2). Samples x-546, x-700, x-705, 82, 102, kam-2, x-733–2 have been collected from pre-unconformity successions (points (3) and (4) in Section 3.1), reflecting pre- and synorogenic stages of the CTB evolution, while samples 82,101, x-531 were collected from a post-orogenic unit above the regional angular unconformity (point (5) in Section 3.1) (Figure 2). The simplified stratigraphic column (Figure 3(a)) is modified using regional stratigraphic nomenclature of Proskurnin *et al*. (2016, accepted).

The Mesoproterozoic Oktyabr' Formation (ok in Figure 3(a), sample x-546) is up to 2000 m thick succession of light-grey, locally cross-bedded quartzite with subordinate phyllite and conglomerate interbeds. Conglomerate pebbles are mainly represented by quartz and quartzite, but some granite and amphibolite are present as well. The Zhdanov Formation is 850–1000 m thick, conformably overlies rocks of the Oktyabr' Formation, and consists of grey phyllites, quartzite, and marbles (Pogrebitsky and Shanurenko 1998; Proskurnin 2009). Together with siliciclastic units often referred to as undefined Mesoproterozoic units (Proskurnin 2009), or carrying names of local stratigraphic subdivisions (Proskurnin *et al*. 2016, accepted), these two Formations form up to 5 km thick Oktyabr'–Zhdanova succession.

The Mesoproterozoic Oktyabr'–Zhdanov succession is cut by Severobyrrang mafic Complex (samples x-700 and x-705). Of the total mafic intrusions, that are generally 20–100 m thick intrusive bodies traced along the strike for up to 30 km, more than 90% are sills, and about 10% are dikes. Though metamorphosed under greenschist facies conditions together with host sedimentary succession, mafic rocks retain primary ophitic texture (Proskurnin 2009). Major oxide contents (Proskurnin 2009) indicate tholeiitic affinity of the Complex; trace and rare earth element geochemical analysis (Supplementary file 6) indicate probable sub-alkaline E-MORB nature of the sill x-700 (Figure 3(c,d)).

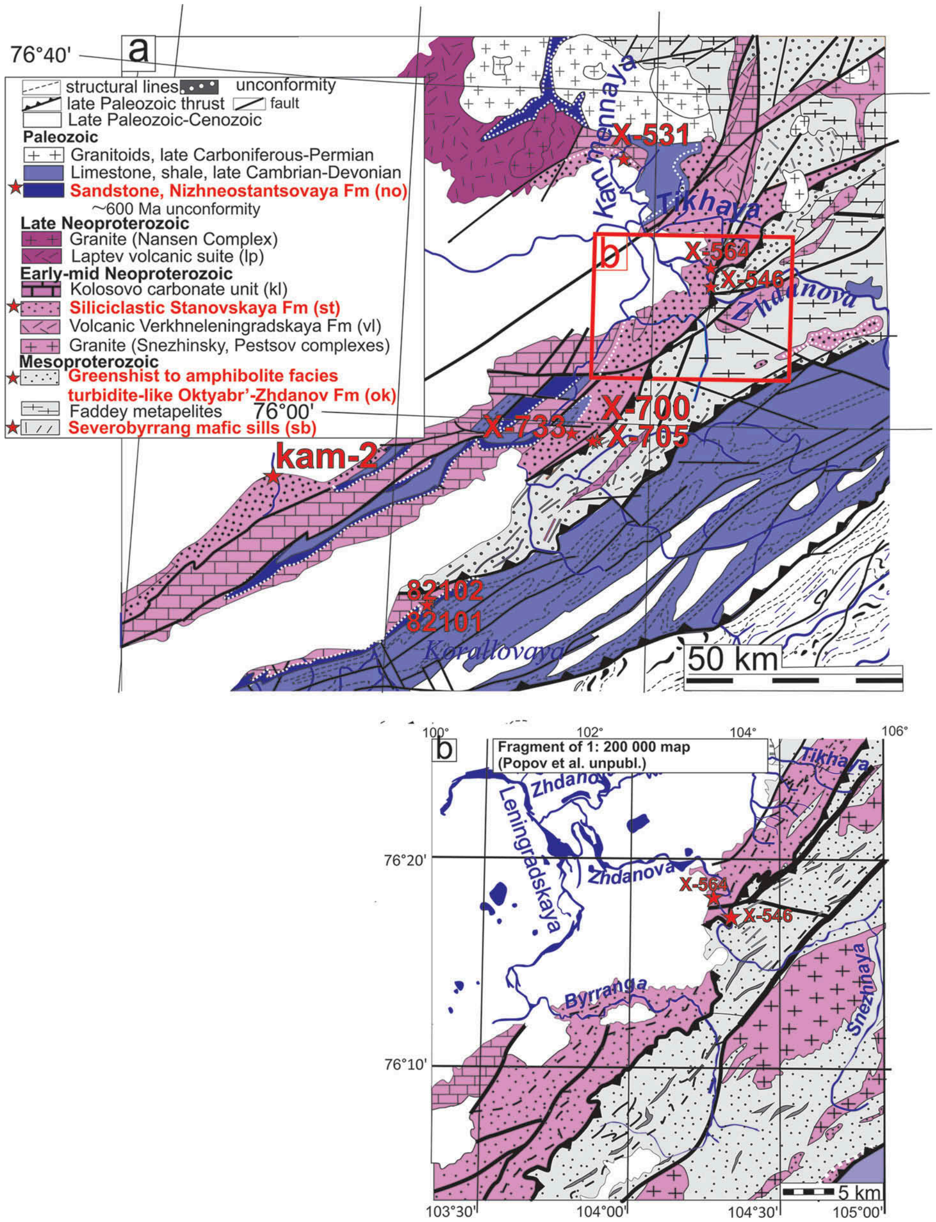

Figure 2. Simplified geological map showing relationship between major geological units in the study area, simplified after Kachurina *et al*. (1998); Makariev and Makarieva (2012); Markovsky *et al*. (2003); Popov *et al*. (unpublished); Proskurnin *et al*. (2009); Proskurnin *et al*. (2014); Proskurnin *et al*. (2016, accepted). The inset map (b) shows the relationship between major geological units in the study area in detail. Stars show sample locations.

The overlying Verkhneleningradskaya Formation (vl in Figures 2 and 3(a)) is more than 250 m thick succession of metamorphosed under greenschist facies volcanic flows and tuffs of predominantly acid compositions, as well as minor metandesite and metabasalts. Volcanic rocks of the Formation share geochemical signature of fractionated I-type magmas with spatially associated Zhdanov and Snezhnisky granitoid complexes (Figure 2). Zircons recovered from metandesite and metarhyolite yield U–Pb zircon age in range of ca. 870–820 Ma (Proskurnin *et al.* 2014), confirming that the volcanic rocks are comagmatic with above mentioned granitoids. Commonly, the Verkhneleningradskaya Formation has faulted contacts with the Oktyabr'–Zhdanova succession (Figure 2(a)), and the similarity in their metamorphic grade and structural style implies that both were subjected to the same Neoproterozoic tectonic event (Proskurnin 2009; Proskurnin *et al*. 2014).

The Stanovskaya Formation (st in Figure 3(a), samples x-733, 82102, kam2) unconformably overlies ca. 850–820 Ma granitoids and metasedimentary rocks of the Oktyabr' and Zhdanova formations (Figure 2),

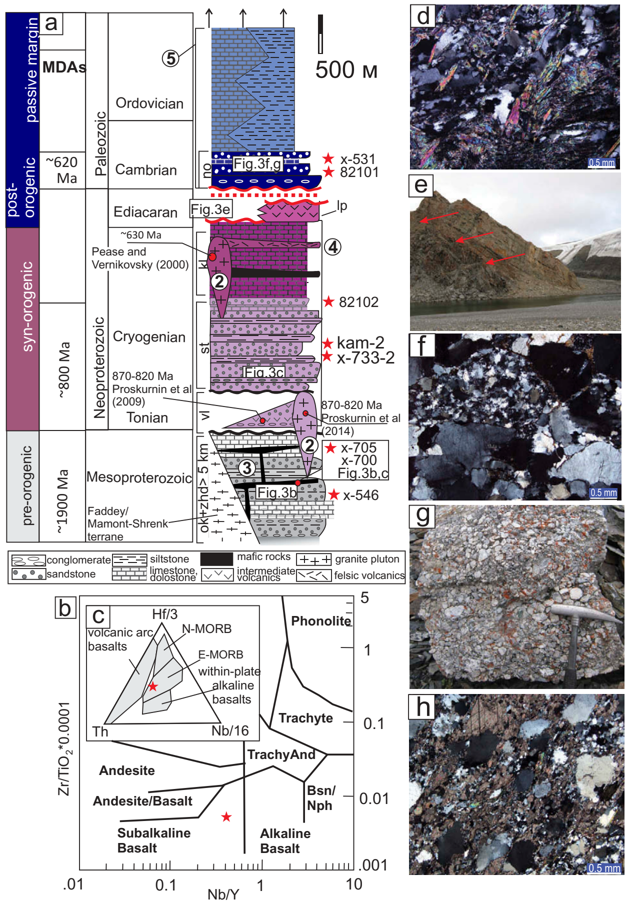

Figure 3. Simplified stratigraphy of the rock units in the study area (a), their composition (b–d, f–g) and field occurrence (e); (b) chemical composition of mafic sill x-700 (data in Supplementary file) on classification diagram after Winchester and Floyd (1977), (c) and discrimination diagram after Wood (1980); (d) microphotograph of quartz schist (x-546) from the Oktyabr' Formation; (e) angular unconformity, that separates deformed Mesoproterozoic greenshist facies Oktyabr' Formation from the Paleozoic succession; (f) microphotograph of lithic arenite (x-733) from the Stanovskaya Formation (g) calcarenaceous conglomerate of Nizhneostantsovaya Formation; (h) microphotograph of calcarenaceous gravelite (x-531) from the Nizhneostantsovaya Formation. Symbols: okt–zhd: Oktyabr'–Zhdanov formations; dr: Dorozhninsk Formation; st: Stanovskaya Formation; kl: Kolosova Formation; lp: Laptev suite; no: Nizhneostatsovaya Formation. Numbers in circles are references in text of Section 3.1.

although faulted contacts are also common (Proskurnin 2009). The Formation is commonly interpreted as molasse (Vernikovsky 1996; Pogrebitsky and Shanurenko 1998), because its siliciclastic units contain fragments of volcanics, probably derived from the Verkhneleningradskaya Formation. The lower part of the Formation is dominated by greyish green sandstone including both arkose and lithic arenite varieties, interlayered with rare conglomerate. In the mid-upper part occur red, cross-bedded sandstone packages (samples 82102 and kam-2) and variegated shale interbeds. Microscope studies reveal that the majority samples from mid and upper parts of the Formation are lithic to sub-lithic arenites. Their frameworks are dominated by quartz grains, as well as fragments of quartzite and quartz-rich schist (Figure 3(f)), indicating that these varieties formed through erosion of sedimentary rocks. Total thickness of the Stanovskaya Formation is estimated as 1200–1500 m.

The Stanovskaya Formation is overlain by an up to 2 km thick limestone and dolostone succession, which incorporates several sedimentary cycles (Proskurnin *et al.* 2016, accepted). The most important member of the succession is the Kolosova Formation (kl in Figure 3(a)) of dominantly carbonate rocks. In the southern part of the study area, the Kolosova Formation incorporates basalt flows, trachyte, eruptive pipes and mafic dikes. U–Pb zircon study of the intrusions showed wide range of zircon ages, including 720 Ma concordant grain (Proskurnin 2009), suggesting a mid-to-late Neoproterozoic age of the Formation, consistent with microfossil records (Pogrebitsky and Shanurenko 1998). In the northern part of the study area (Figure 2(a)), Kolosova Formation is overlain by the 800–1000 m thick Laptev bimodal volcanic suite (Markovsky *et al.* 2003; Kachurina *et al.* 2012; Makariev and Makarieva 2012).

In the CTB, an angular unconformity (Figure 3(e)) separates deformed Meso- and Neoproterozoic rocks from the overlying Paleozoic platformal succession (Figures 1(b) and 2). Its lowermost unit Nizhneostantsovaya Formation (no in Figure 3(a)) contains a 0.4–20 m thick basal clastic unit, which consists of light-grey conglomerate, gravelite, coarse grained quartz-rich sandstone (samples 82,101 and x-531). The matrix of conglomerate and gravelite consists of calcite/dolomite, whereas the pebbles are represented by quartzite and dolomite (Figure 3(g,h)).

3.3. Results of U–Pb and Lu–Hf analysis

3.3.1. Severobyrrang mafic sills from the Oktyabr' Formation (samples x-700, x-705)

Two samples have been dated to identify the age of mafic sill emplacement in the older units of the CTB. Related data table is presented in Supplementary file 5. Sample x-700 had three grains that yielded weighted mean average of 1345 ± 35 Ma (Figure 4(a)). The more precise and consistent result of 1365 ± 11 Ma was based on 17 grains analyzed from sample x-705 (Figure 4(b)).

3.3.2. Oktyabr' Formation (sample x-546)

The sample had 90 single grain analyses, of which 88 were 90–100% concordant (Supplementary file 4). The ages of recovered zircons are predominantly <2200 Ma (Figure 5(a)), and only three grains revealed significantly

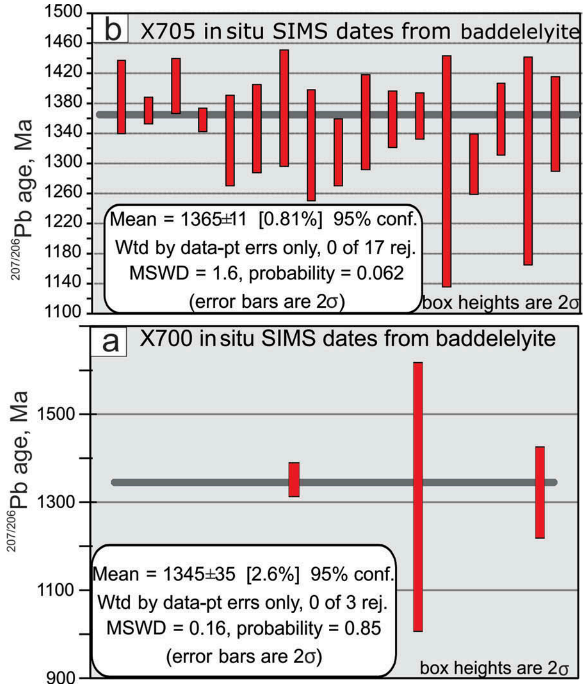

Figure 4. Results of *in situ* SIMS baddeleyite dating of mafic sills x-705 (a) and x-700 (b).

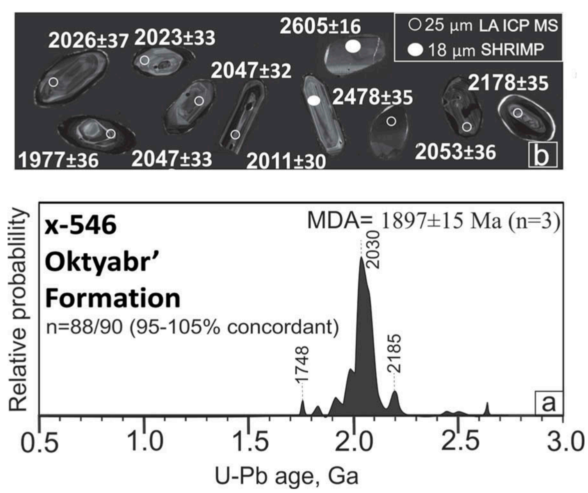

Figure 5. Detrital zircon age spectrum (a) and representative CL images of zircons (b) recovered from the Oktyabr' Formation sandstone.

older ages in range of 2600–2400 Ma. Mid-to-late Paleoproterozoic grains are commonly subrounded, vary in length from 50 to 250 μm and often preserve growth zoning. By contrast, the older grains commonly have featureless, stained or chaotic internal structure with traces of resorption and recrystallization, common of metamorphic zircons (Corfu *et al.* 2003). The main age cluster 2100–1940 Ma (80% of total zircon population) defines the prominent peak at 2030 Ma. Minor peaks at 2180 and 1920 Ma are associated with the 2200–2100 and 1940–1900 Ma age clusters, respectively. Mean age of the youngest cluster is 1897 ± 15 Ma (n = 3, MSWD = 0.58).

3.3.3. *Stanovskaya Formation (samples x-733–2, kam-2, 82,102)*

Three specimens of the Stanovskaya Formation were analysed to obtain detrital zircon age spectra (Figure 6). The sample x-733 had 61 grains analysed (Supplementary files 2 and 3), of which 72 met the 10% discordance criteria, while samples 82102 and kam-2 had 93 out of 103, and 114 out of 117 less than 10% discordant analysis, respectively (Supplementary file 2). The majority of analysed grains from the Stanovskaya Formation plot along the Concordia (Supplementary file 5).

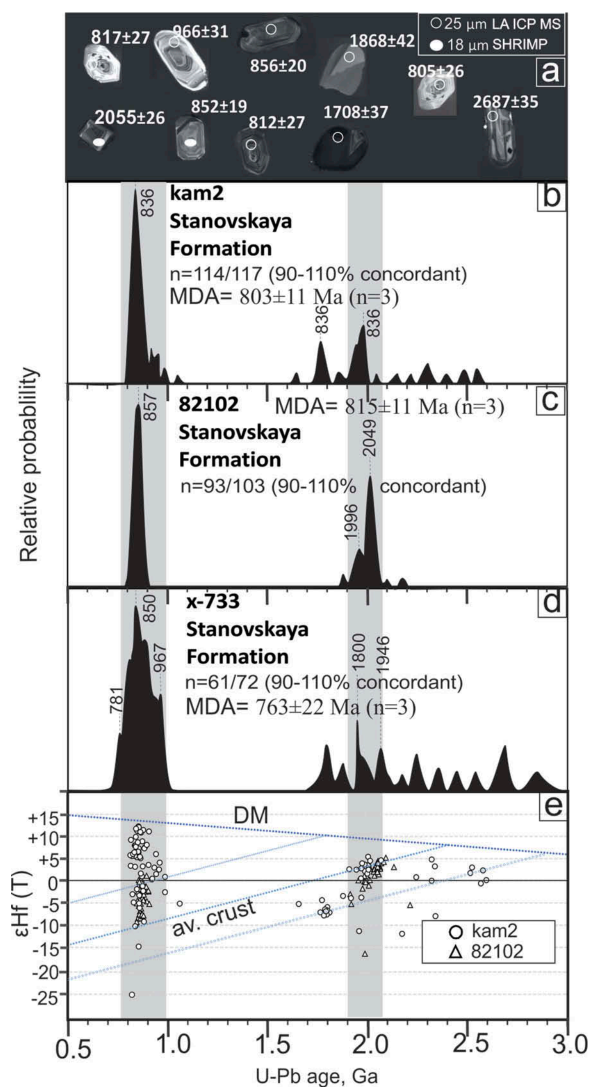

Figure 6. Detrital zircon age spectra (b–d), Hf isotopic compositions (e) and representative CL images of zircons (a) recovered from the Stanovskaya Formation sandstone.

Broadly, all three samples reveal similar detrital zircon age spectra, with a predominant early Neoproterozoic zircon population (up to 61%) and subordinate Paleoproterozoic and Archean populations (Figure 6(b–d)). The early Neoproterozoic zircon population is commonly represented by (50–100 μm) pinkish-coloured, euhedral grains, suggesting derivation from a proximal igneous source (Figure 6(a)). In sample kam-2, the age range of Neoproterozoic zircons is between 970 and 800 Ma, more extended than 900–800 Ma in samples 82102 and x-733.Nonetheless, for all samples a peak at 850–830 Ma is prominent.

The older, early Precambrian grains tend to be subrounded (Figure 6(a)), although about 30% are euhedral. In sample 82102, Paleoproterozoic 2100–1960 Ma age cluster defines the prominent peak at 2050 Ma. In samples kam-2 and x-733, Paleoproterozoic grains distribute into two age clusters: the younger 1820–1740 Ma that defines peak at ca. 1800 Ma, and the older 2100–1960 Ma cluster that has peak at ca. 2000 Ma. Remaining grains are scattered between 1820–1960 Ma, and 2010–3000 Ma.

The MDAs (maximum depositional age) of samples kam-2, 82102 and x-733 are 803 ± 11 Ma (n = 3, MSWD = 0.026), 815 ± 11 Ma (n = 3, MSWD = 0.64) and 763 ± 22 Ma (n = 3, MSWD = 0.58), respectively.

The predominant early Neoproterozoic (900–780 Ma) zircon population forms a strong vertical array on the εHf(T) *versus* age plot (Figure 6(e)), with εHf(T) values falling in range between −10 and +11, except two grains that have εHf(T) values of −15 and −26. The 980–900 Ma old zircons are characterized by εHf(T) values varying from −4 to +6; similarly, the major Paleoproterozoic 2100–1960 Ma zircon population is characterized by εHf(T) values varying from −2 to +6. The majority of Archean grains have εHf(T) values hovering around CHUR.

3.3.4. Nizhneostantsovaya Formation (samples x-531, 82101)

Zircons recovered from sample x-531 consist of ~100–150 μm grains of which ~80% are rounded, and ~20% are prismatic. 53 grains were analysed of which 42 were <10% discordant. The age spectrum of sample x-531 (Figure 7(b)) reveals two Neoproterozoic zircon age clusters: 600–640 Ma (7%) that has a peak at 630 Ma, and 1000–800 Ma (40%) that has a plateaux-like peak at 850–940 Ma. Zircons ages that range between 1000 and 1600 Ma (12%) are uniformly distributed along the spectrum. Significant Paleoproterozoic zircon age cluster is 2110–2010 Ma with peak at 2050 Ma (17%). Archean grains (12%) vary in age between 3500 and 2600 Ma. The MDA based on mean age of the youngest

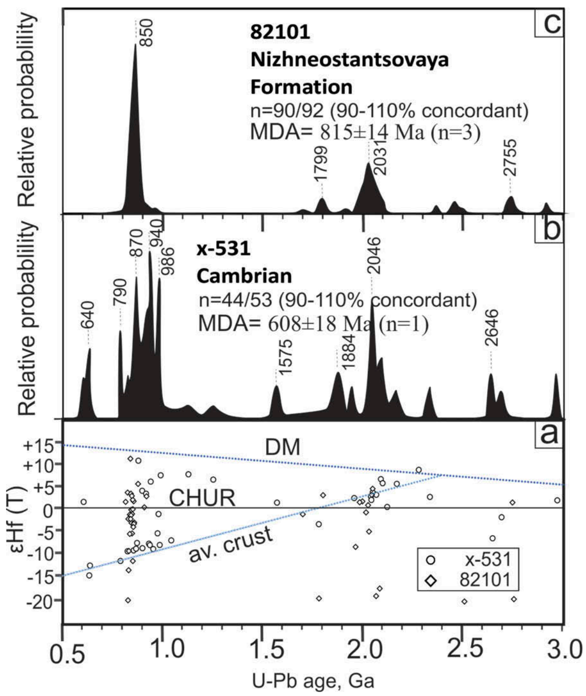

Figure 7. Detrital zircon age spectra (a and b), Hf isotopic compositions (c) of zircons recovered from the Nizhneostantsovaya sandstones.

cluster is 627 ± 44 Ma (n = 3, MSWD = 3.4) and based on the youngest single grain (YSG) age, it is 608 ± 18 Ma, overlapping at ~620–600 Ma.

The age spectrum of the second sample 82101 (Figure 7(c)) from the Nizhneostantsovaya Formation and the sample 82102 of the Stanovskaya Formation share prominent ca. 870 Ma peak. In both samples the early Neoproterozoic zircon population forms a strong vertical array on the εHf(T) *versus* age plot (Figure 8(a)), with εHf(T) values falling in range between −10 and +12 and only four grains with εHf (T) values <−10. The 2010–2110 Ma zircon populations is also by relatively juvenile εHf(T) values, clustering between +8 and −1.

4. Precambrian of the Siberian platform

4.1. The sedimentary cover of the SC

Sedimentary units of the SC broadly form two distinct sedimentary successions separated by a major late Ediacaran unconformity, defined by seismic and geological data (e.g. Vernikovsky *et al.* 2004; Melnikov *et al.* 2005; Sovetov *et al.* 2007; Frolov *et al.* 2015). The unconformity is inferred to represent a Neoproterozoic hiatus, which lasted for 200 My and locally for up to 400 My (Gladkochub *et al.* 2009). The Neoproterozoic hiatus in the northern part of the platform relates with timing of

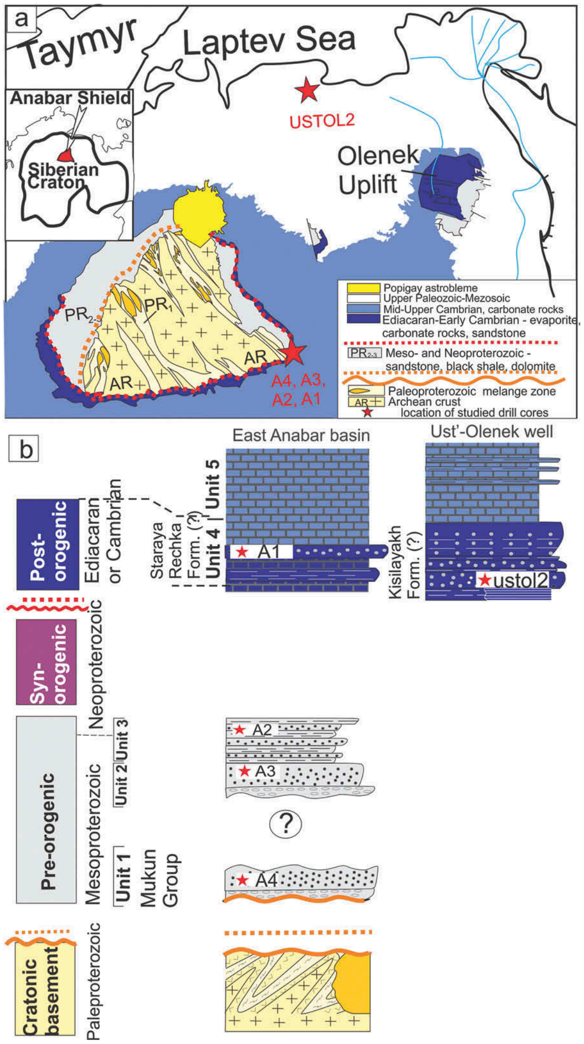

Figure 8. Geological and stratigraphic setting of samples collected from the Siberian platform cover.

the CTB formation. The samples A4, A3, A2, A1, and ustol 2 (Figure 8) were analysed to characterize changes in sedimentary provenance that may have occurred in response to accretion of the CTB. Samples A4, A3, A2 were collected from below, and sample A1 from above the major unconformity. The ustol 2 sample is a potential age correlative with A1 (Figure 8).

Meso- to early Neoproterozoic 'pre-unconformity' sedimentary rocks are widely distributed on the SC within rift-related, intracratonic sedimentary basins (Semikhatov and Serebryakov 1983; Melnikov, 2005; Frolov *et al*. 2015). In these basins, fluvial to shallow marine sedimentation followed intracratonic extension associated with emplacement of Mesoproterozoic mafic dike swarms (Gladkochub *et al*. 2010, and references therein), which in turn followed a number of Paleoproterozoic collisional events that terminated by 1.8 Ga (Rosen 2003).

One of such basins established on top of early Precambrian crust of the northern SC is the east Anabar basin (Figure 8). Samples A4, A3, and A2 were recovered from drill cores and described in detail by Kuptsova (2012) and Kuptsova *et al*. (2011, 2015)) presumably as a part of Meso–early Neoproterozoic succession (Kuptsova 2012; Kuptsova *et al*. 2015), which overlies the Archean and Paleoproterozoic basement of the eastern Anabar Shield (Figure 8(b)) and contains its erosional products (Kuptsova *et al*. 2015; Priyatkina *et al*. 2016). Here we present Hf in zircon data for previously analysed detrital grains (Kuptsova *et al*. 2015; Priyatkina *et al*. 2016). Sample A1 comes from clastic unit which makes a part of dolomitic unit 4 of the East Anabar basin (Kuptsova *et al*. 2011). Lithologically, sample A1 differs from the underlying fluvial units, as it consists of grey subarkosic sandstone interbedded with carbonate horizons. Presumably, it belongs to the Ediacaran Staraya Rechka Formation (Kuptsova *et al*. 2015) (Figure 8). In the stratotype, the Formation has a clear erosional surface at the base. Sample ustol 2 was recovered from drill core of the Ustolenekskaya well, located near the Laptev Sea (Figure 8). The sample is represented by lithic gravelite, collected from a 100 m thick siliciclastic package that presumably belongs to the Kisilayakh Formation of the Kenkil Group. The framework is poorly sorted, contains as much as 70–80% lithic fragments, 5–10% feldspar, and 15–30% quartz grains. An Early Cambrian age has been suggested for this unit based on the palaeontological record and the youngest detrital zircon grain age of 530 ± 3 Ma (Kochnev *et al.* 2013).

4.2. Results of U–Pb–Hf detrital zircon study

4.2.1. Samples A4, A3, A2: SC fingerprint

Detailed description of U–Pb data used for further Hf in zircon work is presented in Kuptsova *et al*. (2015) and Priyatkina *et al*. (2016). Combined, the three samples from lower part of the east Anabar basinal succession reveal a common Paleoproterozoic zircon age cluster with peaks at ca. 2050 and 1950 Ma, respectively (Figure 9(a)). For the majority of the 2120–2000 Ma grains, calculated εHf(*T*) values are positive, varying from +1 to +8.5, although a few grains have negative εHf(*T*). The 2000–1900 Ma old zircons show much larger εHf(*T*) variations from −27 to +3, with majority of values ranging from −20 to +8. εHf (*T*) values of Archean grains from all samples are mostly clustered between 0 and +6.

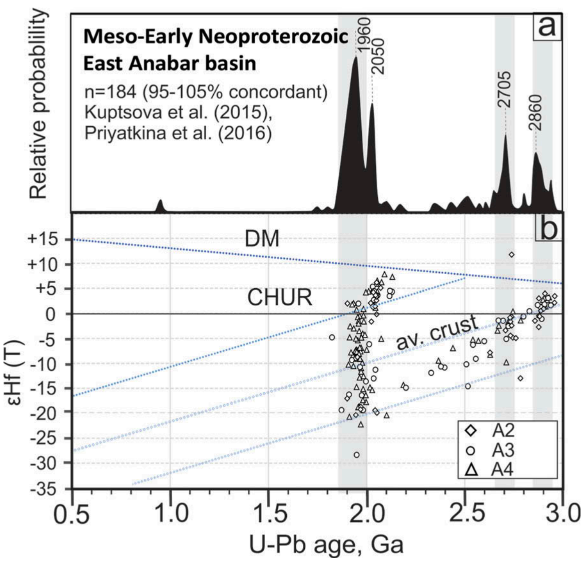

Figure 9. Combined detrital zircon age spectrum (a) for Meso- and early Neoproterozoic sandstones A4, A3, A2 from the East Anabar basin (Priyatkina *et al.* 2016), Hf isotopic compositions of zircons (b).

4.2.2. Ediacaran–Early Cambrian: post-orogenic signature of northern SC

The zircons recovered from the sample A1 are dominantly ~100–300 μm long clear subrounded prisms, although up to 30% grains are rounded. Of the 123 analysis, 103 were <10% concordant. The predominant zircon age cluster is 2160–1910 Ma (22% of total population) with probability peak at 1960 Ma, although Paleoproterozoic grains with ages that range between 1900–1700 and 2160–2500 Ma are also present. Another significant age cluster is 680–500 Ma (23%), which defines an age peak at 610 Ma. The sample also contains several grains of Mesoproterozoic age (7%), as well as three grains with ages of 950–920 Ma. Archean grains (22%) are scattered along the age spectrum within the interval of 2950–2500 Ma, and two grains as old as ca. 3500–3450 Ma are present as well (Figure 10). The MDA based on the mean age of the youngest cluster is 543 ± 23 Ma (n = 3, MSWD = 2.1), and the youngest single grain age (YSG) is 501 ± 12 Ma.

The zircon population recovered from sample ustol2 is represented by clear ~50–300 mμ long grains, of which ~70% are rounded to subrounded, and ~30% are subhedral, retaining prismatic shape and frequently facets. Of the 100 analysis, 93 were <10% concordant. The detrital zircon age pattern (Figure 10(b)) is dominated by a ca. 720–560 Ma zircon population (66% of total population) that defines a prominent peak at 680 Ma. Other Neoproterozoic grains have ages of 761 ± 25, 813 ± 39, and 830 ± 26 Ma. The sample contains few Mesoproterozoic grains (4%) with ages of 1079 ± 54, 1333 ± 48, 1339 ± 44, and 1442 ± 49 Ma. The remainder of the population comprises 2800–2650 Ma (8%), 2100–1900 Ma (14%) and a few 1900–1600 Ma old zircons. The MDA determined of the youngest cluster is 576 ± 4 Ma (n = 3, MSWD = 0.77) and the YSG age is 572 ± 12 Ma.

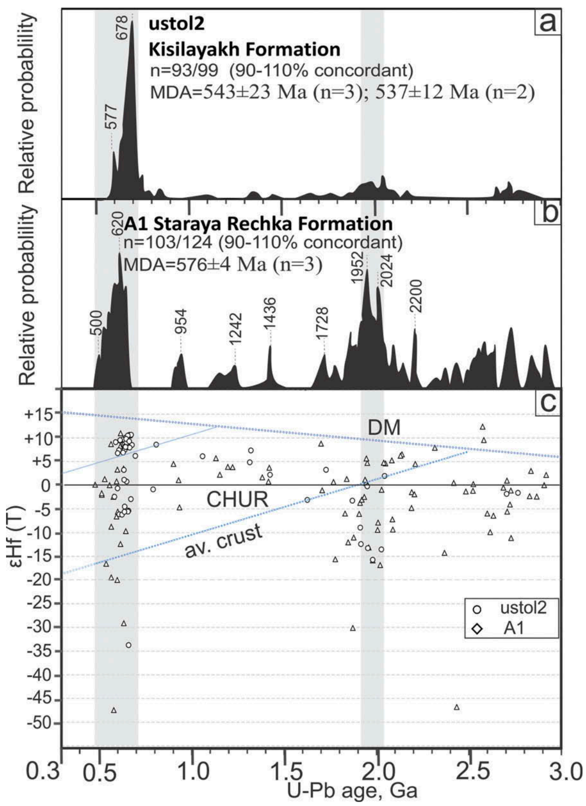

Figure 10. Detrital zircon age spectra (a and b) for earliest Cambrian sandstones from the East Anabar basin and Ust-Olenek well (samples A1 and ustol2), and related Hf in zircon data (c).

The late Neoproterozoic 720–570 Ma age cluster of the two samples A1 and ustol2 outline a strong vertical array with the majority of εHf(T)values ranging between −10 and +11, and few extending to −48 (Figure 10(c)). Further, all samples show trace (<10% of total zircon population) Mesoproterozoic signature, potentially linked genetically with the latest Paleoproterozoic (1.9–1.6 Ga) grains, that are broadly absent from other samples. All together, these have Hf isotopic compositions that plot between CHUR and DM proxies, filling in the field of mantle sources. Hf isotopic compositions of Paleoproterozoic grains in samples of latest Neoproterozoic to Early Cambrian rocks broadly resemble those typical of samples A4, A3, A2 (see Figure 9(b)).

5. Detrital zircon signatures of Meso-to-Neoproterozoic sedimentary basins of northern Siberia and the CTB: summary and comparison

The data reported here help to better constrain the regional stratigraphic correlations, and the provenance of Proterozoic and Early Cambrian sedimentary rocks of the CTB and northeastern part of the Siberian platform (Figure 11).

In the CTB, the oldest dated unit is the Oktyabr' Formation. Its deposition occurred later than 1900 Ma (Figure 5) and was followed by emplacement of the Severobyrrang tholeiitic sills at 1365 ± 15 Ma (Section 3.3.1, Figure 4). The Formation is a part of the siliciclastic-carbonate Oktyabr'–Zhdanov Group, which is locally up to 4 km thick (Proskurnin *et al*. 2009). Significant thickness, medium to fine grained siliciclastic and carbonate lithologies, maturity of the clastic components, large gap between MDA and sedimentation age, embedding of copper-bearing shale units and tholeiitic basalt flows (Proskurnin 2009), indicate that the succession accumulated along a Mesoproterozoic passive margin or an intracratonic rift basin.

Detrital components of the Oktyabr' Formation are erosional products of 2100–1950 Ma magmatic and metamorphic suites (Figure 5). Sedimentary rocks of

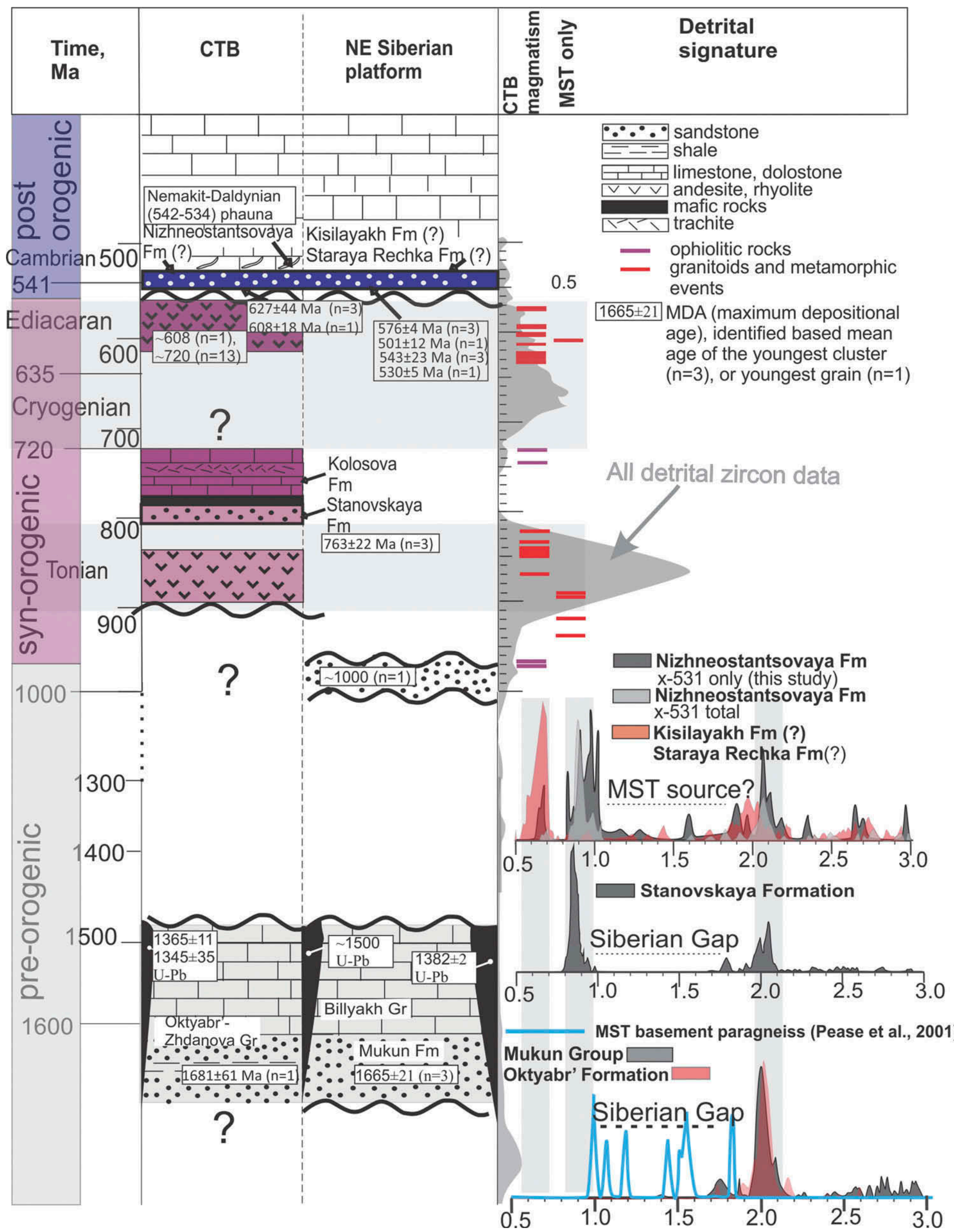

Figure 11. A comparative chart showing the evolution of sedimentary basins in the Central Taimyr Belt (CTB) and northeastern part of the SC (Siberian Craton). CTB chart compiled based on results of this study and references given in Section 3; NE Siberian platform chart modified from Khudoley *et al*. (2015). Source data for magmatism barcode and references are given in Supplementary file 7. Source data for Mukun Group are samples 514–2, 571, 678 from Khudoley *et al*. (2015) and A4 from Kuptsova *et al*. (2015) and Priyatkina *et al*. (2016). Fm: Formation; MST: Mamont-Shrenk terrane.

the same age (Khudoley *et al*. 2015; Kuptsova *et al*. 2015; Priyatkina *et al*. 2016) occur in the Mesoproterozoic intracratonic sedimentary basins, established on top of extended early Precambrian SC crust near the Anabar Shield (Figure 7). About the same time as Oktyabr'–Zhdanov Group was intruded by the Severrobyrrang sills, sedimentary units of the Mukun and Billyakh Groups were intruded by Chieress dikes (ca. 1380 Ma, Ernst *et al*. 2000), suggesting a possibility of correlation between both sedimentary successions and mafic events (Figure 11).

Another succession of regional importance is the Stanovskaya Formation. Timing of its accumulation corresponds to prolonged Neoproterozoic hiatus in the northern part of the Siberian platform (Figure 11). Previously, the age of the Stanovskaya Formation has been constrained between 780 and 650 Ma (Pogrebitsky and Shanurenko 1998; Proskurnin 2009). MDAs obtained for the three samples of the Formation overlap at ~800 Ma, consistent with these estimates (Figure 6 (b–d)).

The Early Neoproterozoic interval of the combined Stanovskaya Formation detrital age spectrum is comparable with early Neoproterozoic flare-up of the CTB magmatism (Figure 11). Euhedral grain shape of recovered detrital zircons (Figure 6(a)), lithic arenite composition and immature texture of the Stanovskaya rock samples (Figure 3(f)) indicate that the sources of clastic material were located near the deposition area and therefore most likely represented a part of the CTB. In this scenario, the major 900–800 Ma and the minor970–900 Ma zircon populations from the StanovskayaFormation (Figure 6) reflect duration of the CTB magmaticsystems, more extended than previouslythought (bar on Figure 11).

The youngest sampled studied stratigraphic unit was the post-orogenic siliciclastic rock association (Figures 3 (a), 8), overlying the unconformity surface on the CTB, and forming the bottom of the Paleozoic sedimentary cycle on the northern SC platform. In the CTB, it is represented by the Nizhneostantsovaya Formation. In the upper part of the Nizhneostantsovskaya Formation, a limestone unit contains fauna, characteristic of Nemakit-Daldyn regional stage (Pogrebitsky and Shanurenko 1998; Proskurnin 2009), i.e. earliest Cambrian (ca. 542–534 Ma, Gradstein and Ogg 1996; Amthor *et al*. 2003). The ~620 Ma MDA of the Formation is slightly older than the sedimentation age, estimated from palaeontological records.

The sandstones of the Nizhneostantsovaya Formation are rich in angular rock and grain fragments, indicating contribution of detritus from proximal sources (Fig. 3 g and h). Some of the sandstones, exemplified by the sample 82101, may have formed through recycling of the underlying (Fig. 3a) metasedimentary basement, as evident from identity of detrital zircon age spectra of the Nizhneostantsovaya and Stanovskaya formations (compare Fig. 6 b, c and d with Fig. 7c). Another sample (x-531) bears a late Neoproterozoic, but also a rare to the CTB and the SC (Fig. 11) population of juvenile Mesoproterozoic and early Neoproterozoic zircons with evolved Hf isotope compositions (Fig. 10, 12). One potential source of the Mesoproterozoic detrital zircons is the MST (Fig. 2b), considered as fragment of non-Siberian origin within the CTB (Pease et al. 2001). Associated with zircons-potential remnants of late Neoproterozoic CTB igneous suites (Fig. 11), erosional products of the MST may also occur in the post-unconformity sandstone of the east Anabar basin (A1), which has numerous zircon ages falling in Mesoproterozoic interval of the detrital spectrum (compare Fig. 7b and 10b).

In the northern Siberian platform, potential age correlatives of the Nizhneostantsovaya unit are samples recovered from the drill cores near the Anabar Shield and the Olenek Uplift. The studied rocks are characterized by late Ediacaran MDAs (n = 3) and Early Cambrian YSG ages, and their minimum depositional age is broadly constrained by late Vendian (Nemakit-Daldynian) limestone units (Figure 11). They have been considered as correlatives of the Kisilayakh and Staraya Rechka formations, although the relationship between the sampled units and the stratotype (e.g. Melnikov *et al*. 2005) has not been reliably established. The new YSG ages may also imply that the correlation of drill cores to the stratotypes was incorrect, or that the age of Staraya Rechka and the Kisilayakh Formations is Early or even Mid Cambrian, younger than previously thought.

The very immature Kisilayakh sandstone and other Early Cambrian lithic arenites of northeastern SC sourced from the extension of the CTB beneath the Laptev Sea (Khudoley *et al*. 2015) provide evidence for prolonged magmatism between 720 and 550 Ma in the orogenic belt. In some of the rock samples, grains as young as 530–500 Ma (Kochnev *et al*. 2013, this study) are present, suggesting that the magmatism in the northeastern Siberia ceased only by the mid Cambrian, when bimodal volcanic rock association (Prokopiev *et al.* 2016) of the Olenek Uplift was emplaced .

6. Hf isotopic evolution of the northern SC margin

A critical aspect of this paper is to establish the cratonic affinity of the Taimyr orogen. Previously, U–Pb–Hf analysis of detrital zircons has been used to characterize the cratonic affinities of specific orogenic belts (e.g. Bahlburg *et al.* 2011; Abati *et al.* 2012; Shi *et al.* 2013; Henderson *et al.* 2016; Wang *et al.* 2016b). The main advantage of using detrital zircon over igneous samples is the ability to obtain a statistically larger dataset of a U–Pb zircon age *versus* εHf(*T*), expressed as Hf arrays, which becomes particularly important when inferring arc-related magmatic systems. This becomes possible through identification of the following phenomena and their interaction: (1) fertilization the lower crustal reservoir with slab-derived fluids and melts, ultimately leading to isotopic modification of crustal signatures expressed via mixing of mantle-like and crustal-like sources, coinciding with vertical isotopic εHf excursions, (2) defertilization of the lower crustal reservoir during roll-back events, coinciding with positive εHf(*T*) excursions as input of juvenile material increases. We further aim to establish the basement affinity of the CTB by comparing detrital zircon populations established on the northern SC prior to and after CTB accretion, and discussing the evidence of geological relationship evidence.

6.1. The isotopic fingerprint of northern SC margin

In contrast to many other cratons, the Precambrian basement of the SC lacks Mesoproterozoic crust (Rosen *et al.* 1994; Rosen 2003; Glebovitsky *et al.* 2008). This is reflected in the zircon population from the Meso- to Early Neoproterozoic sedimentary platformal units of the East Anabar basin, which directly overlie basement domains within the northeastern SC (Khudoley *et al.* 2015; Kuptsova *et al.* 2015; Priyatkina *et al.* 2016). Recovered detrital zircons group into distinct populations at 2.9–2.7 , 2.15–2.0, and 2.0–1.9 Ga (Figure 9, Kuptsova *et al.* 2015, Priyatkina *et al.* 2016). εHf(*T*) values of the younger Paleoproterozoic (2.0–1.9 Ga) Siberian zircon population range from −20 to +7 (Figures 9(b) and 12(a)), forming an extended vertical

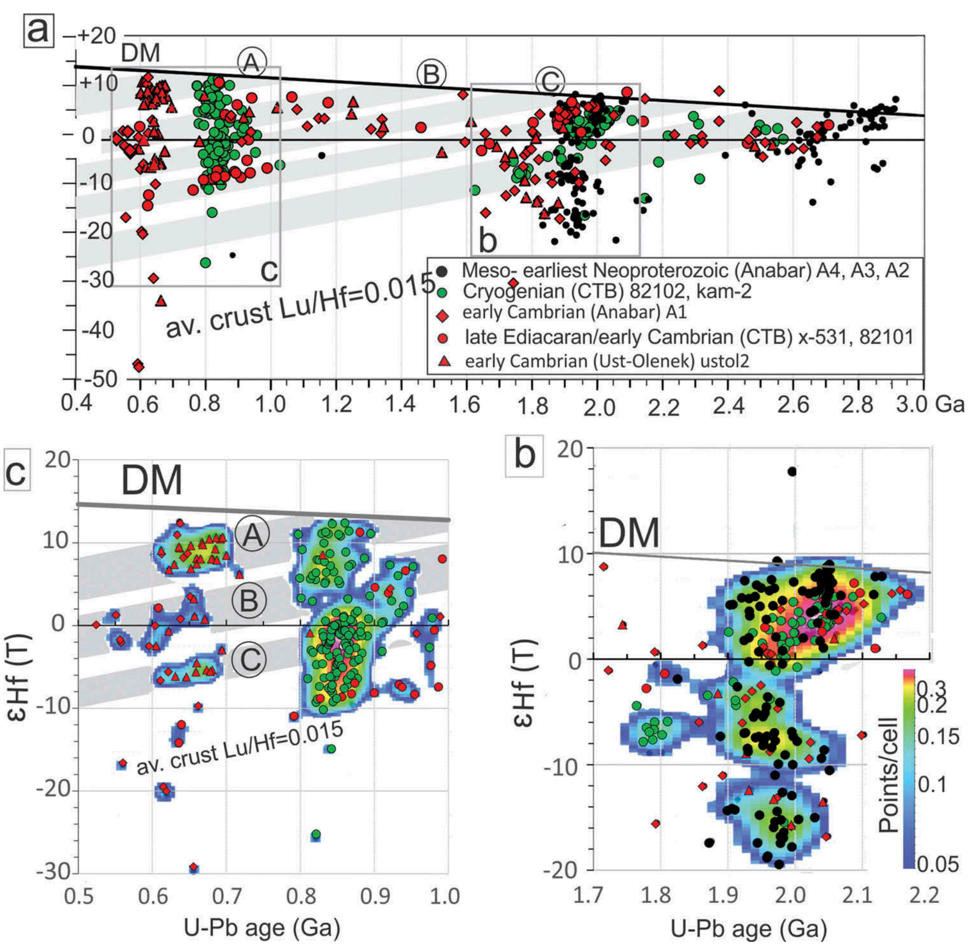

Figure 12. Hf isotope compositions vs. U–Pb age plot for detrital zircons recovered from sedimentary rocks of northern Siberia (a). Insets (b) and (c) are enlarged plots of Paleoproterozoic and Neoproterozoic data points, supported by data density plots. Source data are presented in Supplementary file 3. (A), (B), and (C) in circles are evolutionary trends of source mafic underplates with Lu/Hf ~0.015 and likely yielding meaningful (Payne *et al.* 2016) Hf model ages of A ~1000–800 Ma (A), ~1500–1300 Ma (B), 1900–1700 Ma (C).

array. The older (2.15–2.0 Ga) Paleoproterozoic zircon population (Figure 8) is characterized by positive εHf(*T*) values ranging from +2 to +9 (Figure 12(b)), suggesting that the host magma was derived from partial melting of an oceanic arc terrane, or some other form of primitive mafic crust.

6.2. Sources of the CTB Neoproterozoic magmatic systems, and their cratonic affinity

The studied syn- and post-orogenic Neoproterozoic to Early Cambrian rocks (Sections 3.3.3, 3.3.4, 4.2.2) from northern SC and the Taimyr orogen were derived from proximal sources, as evidenced from occasional presence of volcanic fragments, immature textures of rock samples (Figure 3(f–h)), as well as euhedral shape of zircons recovered from them (e.g. Figure 6(a)). Being erosional products of the CTB, these samples can be used to characterize its crustal constituents.

Broadly, U–Pb detrital zircon age spectra of the rocks reveal two main Neoproterozoic peaks at 970–800 and 720–600 Ma ranges (Figure 11), further referred to as the early and late Neoproterozoic peaks. The early Neoproterozoic peak has a low at ~900 Ma, drawing minor 970–900 Ma and major 900–800 Ma zircon populations.

Although few analysis show negative εHf(*T*), the majority of εHf(*T*) values in the 970–900 Ma zircons from the Stanovskaya Formation range between 0 and +8 (Figure 12(a,c)), consistent with εHf(*T*) values of zircons derived from modern and recent arc terranes (Ji *et al*. 2009; Arndt 2013; Wang *et al*. 2016a).

To present knowledge, the major 900–800 Ma zircon population can only be linked with the S- and I-type granitoid belt of the Faddey terrane (Vernikovsky 1996; Vernikovsky *et al*. 1998; Pease and Vernikovsky 2000; Kuz'min *et al*. 2007) and adjacent area (Proskurnin *et al*. 2014), which forms the basement to the Formation. The isotopic information about magma sources of this extensive magmatic belt previously was limited to Nd model ages of ca. 1.9–1.8 Ga (Vernikovsky *et al*. 1996). It has been shown (Arndt and Goldstein 1987) that mixing phenomena impacts significantly on the interpretation of Nd model ages, but the same issue has been for a long time underestimated for Hf model ages, leaving their meaning questionable (Payne *et al*. 2016).

Our Hf in zircon data (Figure 12) provide new information on the complex origin of this magmatic belt. Broadly, the 900–800 Ma zircon population forms a subvertical array in εHf(*T*) space (Figure 12(a)). Its endmember components indicate mixing of a crustal (negative εHf(*T*) endmember) and mantle (positive εHf(*T*) endmember) sources, typical of zircon populations associated with continental arcs (e.g. Griffin *et al*. 2002; Yang *et al*. 2006; Kemp *et al*. 2007, 2009; Linnemann *et al*. 2014; Smits *et al*. 2014). However, a more detailed analysis (Figure 12(c)) indicates that two main clusters of εHf(*T*) values define two main source components of the 900–800 Ma magmatic system. One of them (εHf(*T*) values in range of +4 to +14) is equivalent to mantle, juvenile crust or reservoir 'New Crust' (Dhuime *et al*. 2011). Another cluster (εHf(*T*) values in range of +2 to −10, with maximum point/cell density located between ~0 and −4) defines a crustal source. Within the cluster, significant variability in εHf(*T*) from +2 to −10 suggests that the crustal source itself represents a mixture of components.

Two lines of evidence suggest that the ancient crustal sources, reworked during the ca. 970–800 Ma continental arc magmatism, was the early Precambrian basement of the northern SC. First, the juvenile 2.2–2.0 Ga zircon population is typical of units deposited on the SC prior to the Neoproterozoic accretionary events (Section 6.1), and its abundance within the syn-orogenic Stanovskaya Formation spatially links its deposition to the SC margin. Further, the upper plate role of Siberia during the early-mid Neoproterozoic orogenic events is supported by geological relationships. In the CTB, the extensive 870–820 Ma S- and I-type granitoid magmatic belt is emplaced into the siliciclastic succession of the Oktyabr' Formation, a fragment of the SC passive margin or the Siberian intracratonic rift basin. The fragment is separated from the SC by Paleozoic thrusts, and until the detrital zircon signature of the Oktyabr' Formation was obtained, its cratonic affinity was unknown. 2.15–2.0 Ga zircon population and a Mesoproterozoic gap in the detrital zircon age spectrum of the Formation (Figures 5 and 11) is the fingerprint of northeastern SC near the Anabar Shield (Sections 4.2.1, 5 and 6.1, Figure 11), which constrains the ultimate source of the Formation as the SC. This interpretation is broadly consistent with palaeomagnetic evidence for establishment the Three Sisters Lake arc complex ~500 km outboard the SC (Vernikovsky *et al*. 2011), and helps to resolve dramatically controversial palaeomagnetic evidences for place of birth the 870–820 Ma granitoid belt (Proskurnin *et al*. 2014; vs. Metelkin *et al*. 2012; Vernikovsky *et al*. 2013).

Variable εHf(*T*) values (−30 to +10) of the 720–600 Ma zircon population (Figure 12(a)) are consistent with mixing of mantle and ancient crustal sources, characteristic of active continental margin (e.g. Griffin *et al*. 2002; Yang *et al*. 2006; Kemp *et al*. 2007; Linnemann *et al*. 2014; Smits *et al*. 2014). A detailed plot of εHf array (Figure 12(c)) shows that mixing was not efficient, allowing several distinct source components of the magmatic system to be distinguished. These components are defined by three major clusters of εHf(*T*) values (Figure 12(c)), including (A) cluster of εHf(*T*) values ranging from +6 to +10, possibly equivalent to mantle, juvenile crust or reservoir 'New Crust' (Dhuime *et al*. 2011); (2) cluster of εHf(*T*) values from −3 to +4, equivalent to CHUR; (3) cluster of εHf(*T*) values in range of −7 to −4, equivalent to crustal component or a low Lu/Hf reservoir. Few zircons with εHf(*T*) values below −10 suggest some reworking of the ancient crustal reservoir may have occurred at ~650–600 Ma . In contrast to the 970–800 Ma zircon population, only few data points resemble DM proxy. Three clusters of εHf(*T*) *versus* age data points (A, B, C on Figure 12(c)) yield regression lines of Lu/Hf ~ 0.015, by that limiting variability of possible sources to mafic underplated crust, preserved oceanic plateaux, mafic arc roots, LIP fragments with certain limitations, or the oceanic crust of a passive margin (Payne *et al*. 2016).

The evidences for cratonic affinity of the 720–550 Ma magmatic system are disparate. On one hand, emplacement of ~630 Ma granitoids and ~700–600 Ma HT metamorphism in the ~900–800 Ma peri-Siberian basement (i.e. Faddey terrane, Section 3.1) and apparent north-westward younging of the magmatic systems (Figure 2) favour Siberian affinity of the late Neoproterozoic CTB domains. Juvenile Neoproterozoic basement to the 720–550 Ma igneous suites is also required by Hf evidence for their formation partly at the expense of 1000–800 Ma source (A) equivalent to mafic arc root (Figure 12(c)). Another major source components yield T DM_{Hf} ages of ~1550–1300 Ma (B) and T DM_{Hf} ~1900–1700 Ma (C) may represent LIP fragments of northern SC (Ernst *et al*. 2016), possibly extended (see Section 5) into the northern SC margin as crust of passive margin. These include the 1384 ± 2 Ma Chieress dike (Ernst *et al*. 2000) and the eastern Anabar 1754 ± 27, 1755 ± 22 Ma dike swarm (Ernst *et al*. 2008).

On the other hand, the accretion of exotic terranes to northern SC is also required by the data. Initial evidence comes from Pease *et al*. (2001), who reported abundant 2.6, 1.8–1.0 Ga detritus in a sillimanite gneiss from the MST with MDA of 1004 ± 17 Ma and compared it with the Krummedal succession of east Greenland. Further, our data reveal that an exotic, juvenile late Paleoproterozoic–Mesoproterozoic detrital zircon population, along with ca. evolved 970–900 Ma zircons (red data points on Figure 12(a)), was introduced to the post-unconformity sedimentary rocks of the Siberian platform in the very end of the Neoproterozoic. A tectonic model that allows for both developing the Neoproterozoic arc system on the Siberian margin and for the presence of exotic terranes within the CTB is discussed in Section 8.

7. Accretion of the CTB: a revised tectonic model

The data presented here provide a better understanding of the tectonic processes that took place along the northern margin of the SC throughout the Neoproterozoic. In the following, we discuss five main evolutionary phases of northern Siberian margin during the Neoproterozoic, drawn from integration of U–Pb–Hf detrital zircon and other records.

Phase 0. An active margin near northern Siberia could have initiated through two possible scenarios: collapse of its transform or passive margin, implying subduction initiation beneath oceanic and continental crust, respectively. Generation of zircon-bearing magma began at ~970 Ma, in the transform collapse scenario following either arc maturity, or immediately after slab-flux into the continental margin.

Phase 1. Continental arc near northern Siberian margin allows for lithological diversity and calc-alkaline affinity of the Three Sisters Lake magmatic complex (Section 3) and its emplacement into the Oktyabr'–Zhdanov metasedimentary units of Siberian Mesoproterozoic continental rift/passive margin basin. Generation of zircon-bearing magma in the outer part of the continental margin at 970–900 Ma probably was assisted by slab flux melting of deep crustal zone, and was accompanied by underplating of mafic crust (Figure 13(a)).

Phase 2. Progressive trench retreat promotes extension of the continental arc, allowing for emplacement of S- and I-type granitoids into the Oktyabr'–Zhdanov metasedimentary units of Siberian Mesoproterozoic rift/passive margin basin. Generation of zircon-bearing magmas at 900–800 Ma occurred at the expense of mixed juvenile and mixed evolved material (Figure 12 (c)). Mobilization of evolved sources both in the inner and outer part of the continental margin allowed by decompression and slab flux. Mobilization of juvenile source is progressively increased with slab retreat (Figure 13(b)).

Deposition of the Stanovskaya Formation (ca. 780–700 Ma) followed the accretionary event. Thickness of the Formation locally reaches 1. 5 km; it is widespread, constituting up to 20–30% of the exposed eastern CTB (Kachurina *et al*. 1998; Makariev and Makarieva (2012); Markovsky *et al*. (2003); Proskurnin *et al*. (2009); see also Figure 2). Lithological features of the Formation, such as cross-bedding,

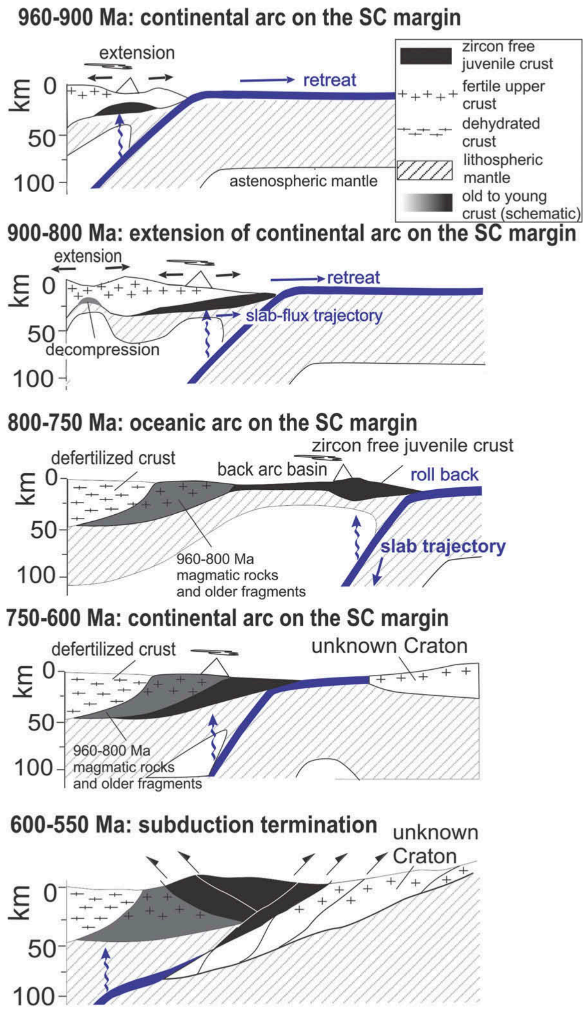

Figure 13. A tectonic model drawn using Collins (2002) shows development of the Central Taimyr Belt (CTB) through five main phases: generation of zircon-bearing magma at 970–900 Ma near the outer part of the continental margin, assisted by slab flux (a); extension of continental arc allows for generation of zircon-bearing magmas at 900–800 Ma at the expense juvenile and evolved material (b) continued roll back results in formation of a back-arc basin, allowing for generation of zircon-free mafic magma over a period of ~800–750 Ma (c); possible underthrusting of the ca. 750–600 Ma back-arc crust and re-establishment of a continental arc through back-arc closure (d) possible underthrusting of a continental lithosphere and termination of subduction zone beneath northern Siberia (e).

presence of conglomeratic horizons, lithic arenite composition and immature textures (Figure 3(f)), indicate that deposition occurred proximal to the source of clastic material. Indicative of convergent plate margin settings (Cawood *et al*. 2012), the ca. 800–760 Ma cluster-based MDAs of the Formation are close to the inferred age of sedimentation based on the presence of mid Neoproterozoic microfossils in carbonates (Pogrebitsky and Shanurenko 1998). All the above-mentioned features indicate that the Stanovskaya Formation was deposited in a large sedimentary basin, most probably in a foreland setting, similar to numerous sedimentary formations of foreland basins in the North American Cordillera (Ingersoll 2008, and references therein). Petrographic evidence of some sedimentary recycling (Section 3.2) suggests that the detrital constituents of the Stanovskaya Formation were more likely sourced from the uplifted accretionary prism, rather than from the underlying volcanic and igneous suites (see Figure 3).

Phase 3. Previously, the ~800–700 Ma interval of the CTB evolution has been considered as rifting stage associated with a break-up of northern Siberia from Rodinia (Vernikovsky and Vernikovskaya 2001), or an island arc formation stage (Vernikovsky 1996; Vernikovsky *et al*. 1996; Metelkin *et al*. 2012; references therein). Entertaining the second option, we suggest that continuation of roll back may have resulted in spreading of a back-arc (Figure 13(c)), allowing for generation of zircon-free mafic magma over a period of ~800–720 or 800–750 Ma. The first estimate is based on the gap in detrital zircon record (Figures 11 and 12), which reliably overlaps with igneous zircon record only at 800–750 Ma. Erosional products of the ~755–730 Chelyuskin and Stanovoy arc suites have not been found in the studied samples, pointing out limitations of this study related to preservation phenomena.

Phase 4. Re-establishment of a continental arc through closure of the back arc basin (Figure 14(d)) allows for emplacement of late Neoproterozoic mafic, intermediate and felsic magmas into the Early Neoproterozoic continental arc fragments (MST and Faddey), and formation of HP metamorphic assemblages near their fringes (Section 3.1). Subduction and subsequent reworking of the back arc crust allows to produce the lithologically complex Chelyuskin and Stanovoy volcanic suites at ~750–730 Ma, consistent with interpretation of Vernikovsky *et al*. (1994). Underthrusting of the ca. 750–600 Ma back-arc magmas accounts for long-term mobilization of a juvenile source with Lu/Hf~0.015 and Neoproterozoic Hf model age (Figure 12(c)), but the role of sources with Hf model ages of ~1.9–1.7 Ga and ~1.5–1.3 Ga and Lu/Hf ~0.015 remains for further consideration (Figure 13(d)).

Phase 5. Underthrusting of a continental lithosphere beneath the northern margin of Siberia may have promoted migration of fluid flux inboard the craton and subsequent melting of dehydrated old crust at 600–550 Ma (Figure 13(e)). Most important, termination of subduction zone beneath northern SC allows for the formation of a major unconformity over northern SC,

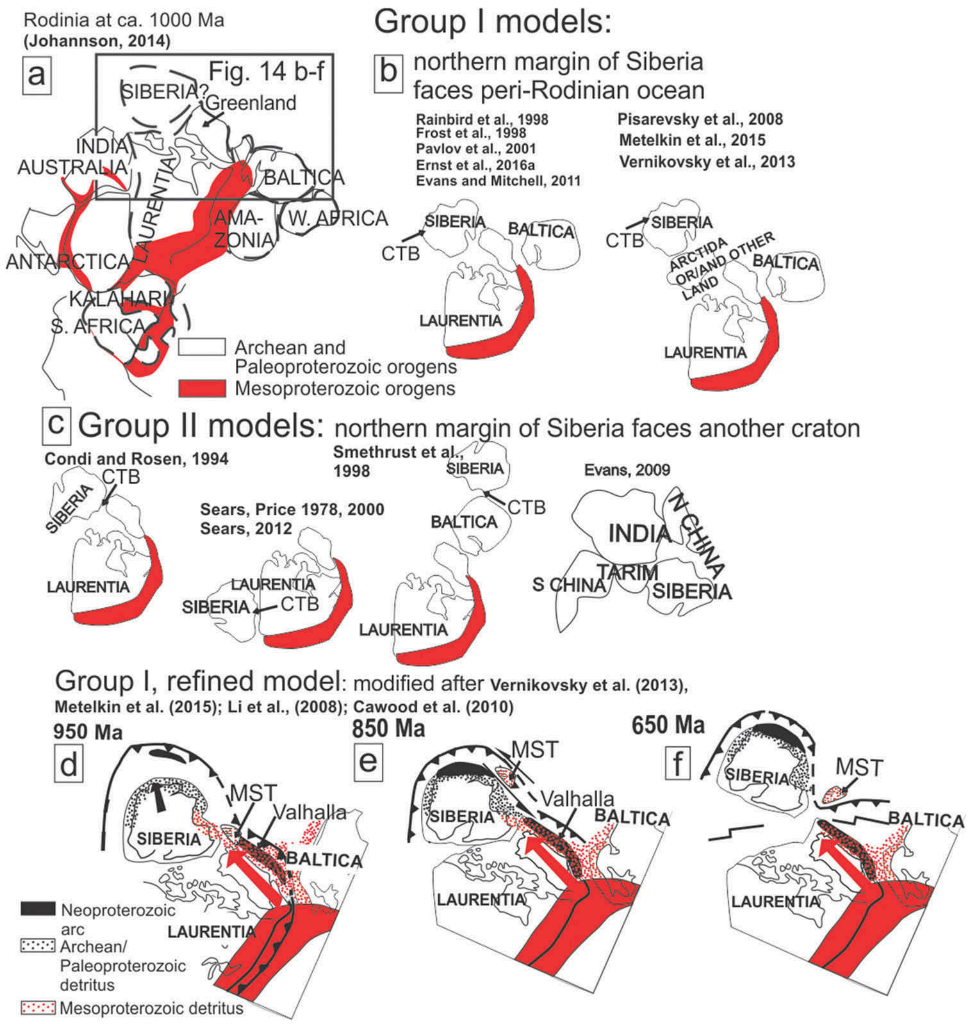

Figure 14. Various models of Laurentia–Siberia–Baltica connection (b–f) within Rodinia supercontinent (a), ca. 1000 Ma. Configuration of Rodinia (a) after Johansson (2014). Other references are on the figure and in text. MST: Mamont-Shrenk terrane; CTB: Central Taimyr Belt.

followed by initiation of a Paleozoic passive margin (Figure 1(b)). However, the age of unconformity surface is yet uncertain: its maximum age is constrained by the ca. 630–615 Ma magmatic and metamorphic events, whereas phaunal remnants recovered from immediately above the unconformity indicate that it can be as young as 534 Ma.

8. Implications for Neoproterozoic supercontinental reconstructions: a test with U–Pb–Hf data

8.1. Implications for Rodinia reconstructions

Broadly, Rodinia models that consider position of the SC can be subdivided into two groups (Figure 14(a–c)). Group 1 models (Frost *et al*. 1998; Rainbird *et al*. 1998; Pavlov *et al*. 2000; Li *et al*. 2008; Pisarevsky *et al*. 2008; Evans and Mitchell 2011; Metelkin *et al*. 2012; Ernst *et al*. 2016) maintain that Siberia was a promontory of Rodinia (Figure 14(a)) and its northern margin faced a peri-Rodinian ocean (Figure 14(b)). Some of the Group II models (Figure 14(c)) also suggest that the SC was a promontory of Rodinia. However, in these models the present-day northern SC margin is juxtaposed to other cratons, such as North China (Evans 2009), Laurentia (Condie and Rosen 1994; Sears and Price 2000; Sears 2012), Baltica (Smethurst *et al*. 1998).

Only the Group I models are supported by this study, because the presented data require that an open ocean existed near the northern margin of the SC at ca. 970 Ma, when the active margin initiated, as evidenced by first early Neoproterozoic supra-subduction magmatic episodes (Vernikovsky *et al*. 2011), also reflected in the detrital zircon record of the northern SC.

Consistent with configurations suggested in the Group I models (Figure 14(a,b)), the margins of northern Siberia and northeastern Laurentia share many similarities in their geological evolution at ca. 1000–750 Ma. The fragments of Siberian Mesoproterozoic passive margin or a rift basin are represented by the ca. 1650–1380 Ma Oktyabr'–Zhdanov Group, which comprises up to 5 km thick succession of carbonate and mature siliclastic rock units, supplied from the northern SC. The 1700–970 Ma magmatic gap, characteristic of the overall Proterozoic detrital zircon signature of northern SC margin (Figure 11), indicates that the northern SC margin was a divergent plate boundary throughout the Mesoproterozoic, until the formation of magmatic arcs near the margin commenced at ca. 970 Ma (Vernikovsky *et al*. 2011; Sections 6 and 7).

According to recent interpretations (Cawood *et al*. 2010, see Figure 14(d)), the ca. 1000 Ma metapelitic and metapsammitic suites of the Krummedal succession (Higgins 1988) represent the fragments of rifted northeastern Laurentian margin. Same as the CTB preserves evidence for establishment the continental arc near Siberia at ca. 970 Ma, the Valhalla orogen preserves the evidence for establishment the continental arc near the northeastern Laurentian margin at ca. 980 Ma (Cawood *et al*. 2010). For example, part of the Renlandian event in the Valhalla Orogen (Cawood *et al*. 2010) was folding the Krummedal succession and its analogues into nappe structures, followed by intrusions of 980–920 Ma S- and I-type granitoids (e.g. Kalsbeek *et al*. 2000; Watt *et al*. 2000; see other ref. in Cawood *et al*. 2010). Thus the margins of northeastern Laurentia and northern SC can be seen as a single peri-Rodinian margin, which transformed from passive into active at 980–970 Ma, following the amalgamation of the supercontinent Rodinia. Such phenomenon is typical in supercontinental geodynamics (Cawood *et al*. 2009).

The main point of divergence in Group I models is the proximity of Siberia and Laurentia within Rodinia (Figure 14(b)). Some palaeomagnetic data (Pavlov *et al*. 2000; Evans and Mitchell 2011; Evans *et al.* 2016) indicate that the Mesoproterozoic connection between southern Siberia and northern Laurentia was tight, whereas using different palaeomagnetic evidence Metelkin *et al*. (2012), Metelkin *et al*. (2015), Pisarevsky *et al*. (2008), Vernikovsky *et al*. (2013), Li *et al*. 2008) maintain that there was a gap between the two cratons. The option of tight connection between Siberia and Laurentia has been also supported by other evidence, such as detrital zircon data (Rainbird *et al*. 1998) and correlation of igneous suites (Frost *et al*. 1998; Ernst *et al*. 2016).

We suggest that the enigmatic MST terrane provides additional evidence for the tight link between the Proterozoic margins of northeast Laurentia and northern Siberia. Despite being a part of the CTB, at least since late Neoproterozoic (Section 6.2), the MST cannot represent a fragment of northern Siberian margin, because its metasedimentary basement bears an exotic relative to the SC Mesoproterozoic detrital zircon signature (Figure 11). The Mesoproterozoic signature prompted Pease *et al*. (2001) to compare the MST with the ca. 1000 Ma fragment of northeast Laurentia (the Krummedal succession), which has received abundant detritus from the Grenville-Sveconorwegian orogen (Kalsbeek *et al*. 2000; Watt *et al*. 2000; Cawood *et al*. 2007). Furthermore, the MST incorporates ca. 950–800 Ma and ca. 650 Ma S-and I-type granitoids (Vernikovsky *et al*. 1996; Pease *et al*. 2001, Figure 11), suggesting that it may have been a part of Valhalla orogen (Figure 14(d)), i.e. a part of the Neoproterozoic arc system, established on the basement of the Krummedal succession and its analogues. In this case, the MST has undergone translation of about ~2500 km (Figure 14(d e)) in the Neoproterozoic, parallel to the peri-Rodinian active continental margin. Exercised by strike-slip movements (Figure 14(e)) or oroclinal bending (Figure 14(f)), such translations are common results of oblique subduction (e.g. Debiche *et al*. 1987; Irving *et al*. 1996). A lesser distance is required if the MST was part of the southeastern Siberian margin, which extended between the Taimyr and Valhalla orogens at ca. 1000–750 Ma. The Mesopoterozoic sedimentary rocks of the Uy and the Kerpyl Groups, that occur along the southeastern Siberian margin, are also rich in Mesoproterozoic detritus (see Figure 14(d–f); (Rainbird *et al*. 1998; Khudoley *et al*. 2015), and therefore are comparable to the metasedimentary basement of the MST. However, proximity of the units to Grenville orogen during their deposition is also required by their detrital signatures (Rainbird *et al*. 1998).

8.2. *Implications for Rodinia break-up and relationship with Timanides*

Based on palaeomagnetic and other geological records, Siberia was separated from Rodinia by ca. 750 Ma (Rainbird *et al*. 1998; Shatsillo *et al*. 2006; Li *et al*. 2008; Metelkin *et al*. 2012; Pisarevsky *et al*. 2013; Pavlov *et al*. 2015; Metelkin *et al*. 2015) or by ca. 635 Ma (Li *et al*. 2013), but where it went after the break up with Laurentia remains problematic.

Several models consider the late Neoproterozoic relationship between Laurentia, Siberia and Baltica, or its absence. Group A models (Metelkin *et al*. 2012; Vernikovsky *et al*. 2013; Metelkin *et al*. 2015) imply that the SC was an independent landmass during the late Neoproterozoic (Figure 15(a)). Group B models, i.e. Roberts and Siedlecka (2002), Hartz and Torsvik (2002) suggest that the northern margin of Siberia formed the along-strike extension of present eastern (Uralian) margin of Baltica (Figure 15(b)). According to these models, both margins were surrounded by a subduction zone during the late Neoproterozoic, allowing formation of the Timanian arc near Baltica and the Taimyr arc near Siberia. The concept of an active northeastern Baltican margin at ca. 750–550 Ma was further entertained by Pease *et al*. (2004) and Linnemann *et al*. (2007). Finally, the reconstructions of Segnor *et al.* (1993) and Scotese (2013), referred to as Group C models connect the northern margin of Siberia to eastern margin of Baltica in the earliest Cambrian (Figure 15(c)).

A better understanding of the Proterozoic evolution of the northern SC margin gained by this study allows a test of the above mentioned models. Group A models are supported by the evidence for a peri-Siberian origin of the Neoproterozoic CTB arc system (Section 6.2). However, the transformation of a plate boundary near the northern SC margin from long-term convergent (ca. 970–550 Ma) into long-term divergent or transform (ca. 500–300 Ma, Uflyand *et al*. 1991; Vernikovsky 1996) hardly can be explained if the northern margin of the SC kept facing an open ocean during the Neoproterozoic and most of the Paleozoic (Metelkin *et al*. 2012; Vernikovsky *et al*. 2013; Metelkin *et al*. 2015).

The key issue for testing the Group B and Group C models is the relation between the CTB and the late Neoproterozoic Timanian orogen, which forms a part of the present northeastern and possibly northern Baltican margin (Figure 15(b,c)) at least since Early Cambrian times (Kuznetsov *et al*. 2010, 2014; Miller *et al*. 2011; Pease 2011).

This relationship can be assessed using U–Pb–Hf detrital zircon signatures of the CTB and the Timanides. A comparison (Figure 16) of detrital zircon populations recovered from the Ediacaran arc-derived clastic rocks of the Timanian orogenic belt (Kuznetsov *et al*. 2010), from late Ediacaran to Cambrian sedimentary rocks with inferred Timanian provenance (Lorenz *et al*. 2008; Amato *et al*. 2009; Pease and Scott 2009; Miller *et al*. 2011; Beranek *et al*. 2013), and from coeval rocks of the northern SC, shows they are broadly similar, but also have some differences.

The main difference between the Taimyr and the Timanian detrital zircon datasets is variability in contribution of Mesoproterozoic *versus* Archean and Paleoproterozoic detritus (Figure 16(b,c)). Partly, this contribution may reflect late Neoproterozoic reworking of some localized sources, but more easily can be explained by Paleozoic recycling of Proterozoic sedimentary rocks, that were formed prior to the Timanian orogenic event along the margins of Baltica and Siberia: Mesoproterozoic detritus is typical of the northern and eastern Baltica margin (e.g. Bingen *et al*. 2011; Romanyuk *et al*. 2014), whereas Archean and Paleoproterozoic detrital zircon signatures characterize Mesoproterozoic sedimentary rocks of northern Siberia. In this case, the variability is not related to the late Neoproterozoic orogenic events. Otherwise, the datasets are broadly similar.

The most important similarity is that both orogens sourced distinct 720–550 Ma zircon population (Figure 16(a)), i.e. the Timanian fingerprint (Pease and Scott 2009), providing evidence for possible tectonic affinity between the CTB and the Timanian orogen such as suggested by either Group B or Group C models (Figure 15(b or c)). Further comparison of zircon populations in εHf *versus* age space (Figure 16(d)) again shows that the majority of 720–550 Ma zircons from the CTB and the Timanides share similar Hf isotopic

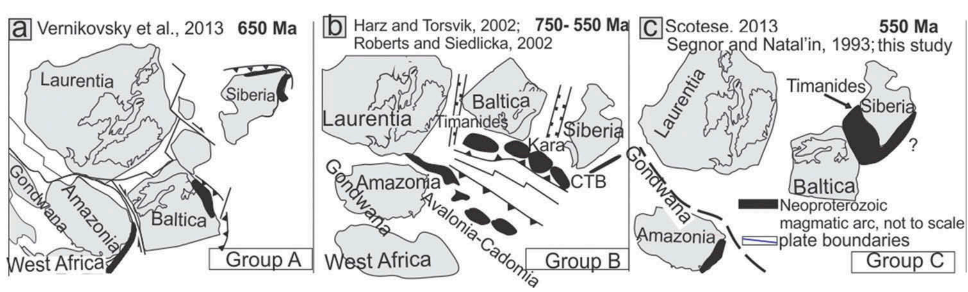

Figure 15. Comparative paleo reconstructions showing possible interactions between Laurentia, Siberia, Baltica and Gondwana in late Neoproterozoic and Early Cambrian: subduction zone along the northern Siberian Craton (SC) is independent (a), modified after (Vernikovsky *et al*. 2013, Metelkin *et al*. 2015); subduction zone along the northern SC is an extension zone of eastern Baltica active margin (b), from Hartz and Torsvik (2002), Roberts and Siedlecka (2002); northern margin of the SC is juxtaposed to eastern margin of Baltica (c), after Scotese (2013). CTB: Central Taimyr Belt.

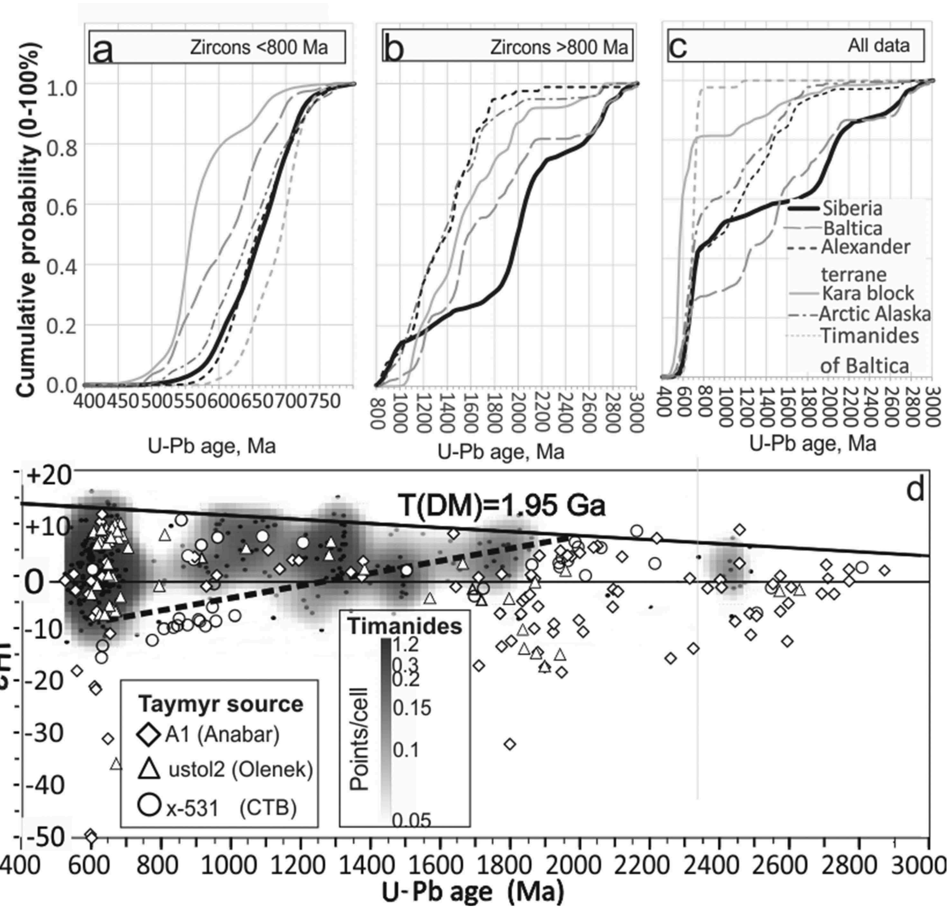

Figure 16. A comparison between U–Pb–Hf detrital zircon records of the Ediacaran and Cambrian rocks sourced from the Timanian arc ('Baltica', 'Kara block', 'Arctic Alaska', 'Alexander terrane', 'Timanides') and the (Central Taimyr Belt (CTB), 'Siberia'). Source data 'Siberia' are from this study, ' Baltica' from Miller *et al*. (2011), 'Kara block' from Pease and Scott (2009) and Lorenz *et al*. (2008), 'Arctic Alaska' from Amato *et al*. (2009), 'Alexander terrane' from Beranek *et al*. (2013). Hf in zircon data for Timanides are from Kuznetsov *et al*. (2010) and Beranek *et al*. (2013). Literature source data for U–Pb detrital zircon cumulative probability plots are given in Supplementary file 7.

signatures. In zircon populations of both datasets, the majority of εHf values extends between +10 and –8. This similarity suggests that the 720–550 Ma zircon populations from the Timanides and the CTB were derived from the arc-related suites, which were not only coeval, but also formed on the same basement, i.e. may represent parts of the same arc system. However, in this interpretation the arc basement cannot be considered to be entirely homogenous, because presence in the CTB dataset of some evolved 650 Ma zircons, with εHf (*T*) as low as –50 (Figure 15(d)) requires melting of local Archean sources.

Where such an arc system could form remains debatable. The similarity of Hf in zircon signatures confronts Group B models (Figure 15(b)), which require that the Timanian and the Taimyr components of the arc system formed on the two different basements: (1) Archean to Paleoproterozoic crust of eastern Baltican margin and (2) the margin of northern SC, which was fringed by an Early Neoproterozoic arc at ca. 750 Ma. In this case, the arc-derived zircons of the CTB and the Timanian orogen should demonstrate a difference in maximum Hf model ages, which is not observed. Further, Kuznetsov *et al*. (2010) argued that the maximum model ages of the 720–550 Ma Timanian population are older than those expected from a Baltican basement. Some crustal components identified in the ca. 720–550 Ma arc system, including that of late Paleoproterozoic Hf model age, mimic those of the Early Neoproterozoic peri-Siberian arc system (Figure 12(c)), suggesting the latter could serve as a basement to the Timanides.

We consider that the broad similarities between detrital zircon signatures of the CTB and the Timanian orogens encourage a re-assessment of the possibility that they represent the two parts of the same orogenic belt (Figure 15(c)). The consideration provides an explanation for the termination of long-lived Neoproterozoic arc magmatism along the northern margin of the SC (Figure 13) by juxtaposition of northern Siberia and northeastern Baltica during the Late Neoproterozoic-earliest Cambrian Timanian orogeny. However, further investigations are needed to fully understand the geodynamic origin of the Timanian orogen, its formation and relationship with Laurentia, Baltica, Siberia, and Precambrian supercontinents.

Acknowledgements

Supported by Australian Research Council Discovery Project 120104004. This article is a contribution of WJ Collins to IGCP648. Thanks to Hui-Qing Huang for his professional guidance during obtaining and processing U–Pb detrital zircon data. Contribution of Vasily Proskurnin is acknowledged. Two reviewers are thanked for constructive reviews.

Disclosure statement

No potential conflict of interest was reported by the authors.

Funding

This work was supported by the Australian Research Council [DP120104004].

References

Abati, J., Aghzer, A.M., Gerdes, A., and Ennih, N., 2012, Insights on the crustal evolution of the West African Craton from Hf isotopes in detrital zircons from the Anti-Atlas belt: Precambrian Research, v. 212–213, p. 263–274. doi:10.1016/j.precamres.2012.06.005

Amato, J.M., Toro, J., Miller, E.L., Gehrels, G.E., Farmer, G.L., Gottlieb, E.S., and Till, A.B., 2009, Late Proterozoic–Paleozoic evolution of the Arctic Alaska–Chukotka terrane based on U-Pb igneous and detrital zircon ages: Implications for Neoproterozoic paleogeographic reconstructions: Geological Society of America Bulletin, v. 121, p. 1219–1235. doi:10.1130/B26510.1

Amthor, J.E., Grotzinger, J.P., Schröder, S., Bowring, S.A., Ramezani, J., Martin, M.W., and Matter, A., 2003, Extinction of Cloudina and Namacalathus at the Precambrian-Cambrian boundary in Oman: Geology, v. 31, p. 431–434. doi:10.1130/0091-7613(2003)031<0431:EOCANA>2.0.CO;2

Arndt, N.T., 2013, The formation and evolution of the continental crust: Geochemical Perspectives, v. 2, p. 405–533. doi:10.7185/geochempersp.2.3

Arndt, N.T., and Goldstein, S.L., 1987, Use and abuse of crust-formation ages: Geology, v. 15, p. 893–895. doi:10.1130/0091-7613(1987)15<893:UAAOCA>2.0.CO;2

Bahlburg, H., Vervoort, J.D., Andrew Dufrane, S., Carlotto, V., Reimann, C., and Cárdenas, J., 2011, The U–Pb and Hf isotope evidence of detrital zircons of the Ordovician Ollantaytambo Formation, southern Peru, and the Ordovician provenance and paleogeography of southern Peru and northern Bolivia: Journal of South American Earth Sciences, v. 32, p. 196–209. doi:10.1016/j.jsames.2011.07.002

Beranek, L.P., Van Staal, C.R., McClelland, W.C., Israel, S., and Mihalynuk, M.G., 2013, Baltican crustal provenance for Cambrian–Ordovician sandstones of the Alexander terrane, North American Cordillera: Evidence from detrital zircon U–Pb geochronology and Hf isotope geochemistry: Journal of the Geological Society, v. 170, p. 7–18. doi:10.1144/jgs2012-028

Bingen, B., Belousova, E.A., and Griffin, W.L., 2011, Neoproterozoic recycling of the Sveconorwegian orogenic belt: Detrital-zircon data from the Sparagmite basins in the Scandinavian Caledonides: Precambrian Research, v. 189, p. 347–367. doi:10.1016/j.precamres.2011.07.005

Cawood, P.A., Hawkesworth, C.J., and Dhuime, B., 2012, Detrital zircon record and tectonic setting: Geology, v. 40, p. 875–878. doi:10.1130/G32945.1

Cawood, P.A., Kröner, A., Collins, W.J., Kusky, T.M., Mooney, W. D., and Windley, B.F., 2009, Accretionary orogens through Earth history. Geological Society, London, Special Publications, v. 318, p. 1–36.

Cawood, P.A., Nemchin, A.A., Strachan, R., Prave, T., and Krabbendam, M., 2007, Sedimentary basin and detrital zircon record along East Laurentia and Baltica during assembly and breakup of Rodinia: Journal of the Geological Society, v. 164, p. 257–275. doi:10.1144/0016-76492006-115

Cawood, P.A., Strachan, R., Cutts, K., Kinny, P.D., Hand, M., and Pisarevsky, S., 2010, Neoproterozoic orogeny along the margin of Rodinia: Valhalla orogen, North Atlantic: Geology, v. 38, p. 99–102. doi:10.1130/G30450.1

Collins, W.J., 2002, Hot orogens, tectonic switching, and creation of continental crust: Geology, v. 30, p. 535–538. doi:10.1130/0091-7613(2002)030<0535:HOTSAC>2.0.CO;2

Condie, K.C., and Rosen, O.M., 1994, Laurentia – Siberia connection revised: Geology, v. 22, p. 168–170. doi:10.1130/0091-7613(1994)022<0168:LSCR>2.3.CO;2

Corfu, F., Hanchar, J.M., Hoskin, P.W.O., and Kinny, P., 2003, Atlas of zircon textures: Reviews in Mineralogy and Geochemistry, v. 53, p. 469–500. doi:10.2113/0530469

Debiche, M.G., Cox, A., and Engebretson, D.C., 1987, The motion of allochthonous terranes across the north Pacific Basin: Geological Society of America Special Papers, v. 207, p. 1–50.

Dhuime, B., Hawkesworth, C., and Cawood, P., 2011, When continents formed: Science, v. 331, p. 154–155. doi:10.1126/science.1201245

Dickinson, W.R., and Gehrels, G.E., 2009, Use of u–pb ages of detrital zircons to infer maximum depositional ages of strata: a test against a colorado plateau mesozoic database, v. 288, p. 115-125 doi:10.1016/j.epsl.2009.09.013

Ernst, R., Buchan, K., Hamilton, M., Okrugin, A., and Tomshin, M., 2000, Integrated paleomagnetism and U-Pb geochronology of mafic dikes of the eastern Anabar shield region, Siberia: Implications for Mesoproterozoic paleolatitude of Siberia and comparison with laurentia: The Journal of Geology, v. 108, p. 381–401. doi:10.1086/314413

Ernst, R.E., Hamilton, M.A., Soderlund, U., Hanes, J.A., Gladkochub, D.P., Okrugin, A.V., Kolotilina, T., Mekhonoshin, A.S., Bleeker, W., LeCheminant, A.N., Buchan, K.L., Chamberlain, K.R., and Didenko, A.N., 2016, Long-lived connection between southern Siberia and northern Laurentia in the Proterozoic: Nature Geoscience, v. 9, p. 464–469. doi:10.1038/ngeo2700

Ernst, R.E., Hanes, J.A., Puchkov, J.A., Okrugin, A.V., and Archibald, D.A., 2008, Reconnaissance Ar–Ar dating of Proterozoic dolerite dykes and sills in Siberia and the southern Urals: Identification of possible new Large Igneous Provinces (LIPs), *in* Proceedings, Common and Regional Problems of Tectonics And Geodynamics, Moscow State University, January 29 – Feb 2, 2008: Moscow Tectonics Conference, GEOS.

Evans, D.A.D., 2009, The palaeomagnetically viable, long-lived and all-inclusive Rodinia supercontinent reconstruction: Geological Society: London, Special Publications, p. 371–404. 327.

Evans, D.A.D., and Mitchell, R.N., 2011, Assembly and breakup of the core of Paleoproterozoic–Mesoproterozoic supercontinent Nuna: Geology, v. 39, p. 443–446. doi:10.1130/G31654.1

Evans, D.A.D., Veselovsky, R.V., Petrov, P.Y., Shatsillo, A.V., and Pavlov, V.E., 2016, Paleomagnetism of Mesoproterozoic margins of the Anabar Shield: A hypothesized billion-year partnership of Siberia and northern Laurentia: Precambrian Research, v. 281, p. 639–655. doi:10.1016/j.precamres.2016.06.017

Frolov, S.V., Akhmanov, G.G., Bakay, E.A., Lubnina, N.V., Korobova, N.I., Karnyushina, E.E., and Kozlova, E.V., 2015, Meso-Neoproterozoic petroleum systems of the Eastern Siberian sedimentary basins: Precambrian Research, v. 259, p. 95–113. doi:10.1016/j.precamres.2014.11.018

Frost, B.R., Avchenko, O.V., Chamberlain, K.R., and Frost, C.D., 1998, Evidence for extensive Proterozoic remobilization of the Aldan Shield and implications for Proterozoic plate tectonic reconstructions of Siberia and Laurentia: Precambrian Research, v. 89, p. 1–23. doi:10.1016/S0301-9268(97)00074-0

Gladkochub, D.P., Pisarevsky, S.A., Donskaya, T.V., Ernst, R.E., Wingate, M.T.D., Söderlund, U., Mazukabzov, A.M., Sklyarov, E.V., Hamilton, M.A., and Hanes, J.A., 2010, Proterozoic mafic magmatism in Siberian craton: An overview and implications for paleocontinental reconstruction: Precambrian Research, v. 183, p. 660–668. doi:10.1016/j.precamres.2010.02.023

Gladkochub, D.P., Stanevich, A.M., Travin, A.V., Mazukabzov, A. M., Konstantinov, K.M., Yudin, D.S., and Kornilova, T.A., 2009, The Mesoproterozoic Udzha paleorift (Northern Siberian Craton): New data on age of basites, straigraphy, and microphytology: Doklady Earth Sciences, v. 425, p. 371–377. doi:10.1134/S1028334X09030052

Glebovitsky, V.A., Khil'tova, V.Y., and Kozakov, I.K., 2008, Tectonics of the siberian craton: interpretation of geological, geophysical, geochronological, and isotopic geochemical data, Geophysical, Geochronological, And Isotopic Geochemical Data: Geotectonics, v. 42, p. 8-20 doi:10.1134/S0016852108010020

Gradstein, F.M., and Ogg, J.G., 1996, A Phanerozoic time scale: Episodes, v. 19, no. 1&2, p. 3-5.

Griffin, W.L., Wang, X., Jackson, S.E., Pearson, N.J., O'Reilly, S.Y., Xu, X., and Zhou, X., 2002, Zircon chemistry and magma mixing, SE China: In-situ analysis of Hf isotopes, Tonglu and Pingtan igneous complexes: Lithos, v. 61, p. 237–269. doi:10.1016/S0024-4937(02)00082-8

Hartz, E.H., and Torsvik, T.H., 2002, Baltica upside down: A new plate tectonic model for Rodinia and the Iapetus Ocean: Geology, v. 30, p. 255–258. doi:10.1130/0091-7613(2002)030<0255:BUDANP>2.0.CO;2

Henderson, B.J., Collins, W.J., Murphy, J.B., Gutierrez-Alonso, G., and Hand, M., 2016, Gondwanan basement terranes of the Variscan–Appalachian orogen: Baltican, Saharan and West African hafnium isotopic fingerprints in Avalonia, Iberia and the Armorican Terranes: Tectonophysics, v. 681, p. 278–304. doi:10.1016/j.tecto.2015.11.020

Higgins, A.K., 1988, The Krummedal supracrustal sequence in East Greenland, *in* Winchester, J.A., ed., Later proterozoic stratigraphy of the northern Atlantic regions: Boston, MA, Springer US, p. 86–96.

Ingersoll, R.V., 2008, Subduction-related sedimentary basins of the USA cordillera, *in* Andrew, D.M., ed., Sedimentary basins of the world, chapter 10: Elsevier, Amsterdam, p. 395–428.

Irving, E., Wynne, P.J., Thorkelson, D.J., and Schiarizza, P., 1996, Large (1000 to 4000 km) northward movements of tectonic domains in the northern Cordillera, 83 to 45 Ma: Jornal Geophysical Research and Solid Earth, v. 101, p. 17901–17916. doi:10.1029/96JB01181

Ji, W.-Q., Wu, F.-Y., Chung, S.-L., Li, J.-X., and Liu, C.-Z., 2009, Zircon U–Pb geochronology and Hf isotopic constraints on petrogenesis of the Gangdese batholith, southern Tibet: Chemical Geology, v. 262, p. 229–245. doi:10.1016/j.chemgeo.2009.01.020

Johansson, Å., 2014, From Rodinia to Gondwana with the 'SAMBA' model—A distant view from Baltica towards Amazonia and beyond: Precambrian Research, v. 244, p. 226–235. doi:10.1016/j.precamres.2013.10.012

Kachurina, N.V., Makariev., A.A., Makarieva, E.M., et al., 2012, Explanatory note to geological map T-45-48 of Russian Federation, cape chelyuskin: St. Petersburg, VSEGEI, 472 p. [In Russian.]

Kachurina, G. N., Lopatin, B. G., Orlov, V. P., Pogrebitsky, Yu. E., 1998, Geological map S 47-49 of Russian Federation, Taimyr series: St. Petersburg, VSEGEI, Scale 1: 1 000 000, 1 sheet. [In Russian.]

Kalsbeek, F., Thrane, K., Nutman, A.P., and Jepsen, H.F., 2000, Late Mesoproterozoic to early Neoproterozoic history of the East Greenland Caledonides: Evidence for Grenvillian orogenesis?: Journal of the Geological Society, v. 157, p. 1215–1225. doi:10.1144/jgs.157.6.1215

Kemp, A.I.S., Hawkesworth, C.J., Collins, W.J., Gray, C.M., and Blevin, P.L., 2009, Isotopic evidence for rapid continental growth in an extensional accretionary orogen: The Tasmanides, eastern Australia: Earth and Planetary Science Letters, v. 284, p. 455–466. doi:10.1016/j.epsl.2009.05.011

Kemp, A.I.S., Hawkesworth, C.J., Foster, G.L., Paterson, B.A., Woodhead, J.D., Hergt, J.M., Gray, C.M., and Whitehouse, M.J., 2007, Magmatic and crustal differentiation history of granitic rocks from Hf-O isotopes in zircon: Science, v. 315, p. 980–983. doi:10.1126/science.1136154

Khudoley, A., Chamberlain, K., Ershova, V., Sears, J., Prokopiev, A., MacLean, J., Kazakova, G., Malyshev, S., Molchanov, A., Kullerud, K., Toro, J., Miller, E., Veselovskiy, R., Li, A., and Chipley, D., 2015, Proterozoic supercontinental restorations: Constraints from provenance studies of Mesoproterozoic to Cambrian clastic rocks, eastern Siberian Craton: Precambrian Research, v. 259, p. 78–94. doi:10.1016/j.precamres.2014.10.003

Kochnev, B.B., Powerman, V.I., and Karlova, G.A., 2013, Concerning the Arctic boundary of the Siberian platform in Cambrian, *in* Proceedings, Common and Regional Problems of Tectonics And Geodynamics XLVII, Moscow

Tectonics Conference: GEOS, Moscow, p. 226–230. (In Russian).

Kuptsova, A.V., 2012, Structure and evolution of uranium-bearing sedimentary basins exemlified by Pasha-Ladoga, East Anabar and Atabaska [Ph.D. thesis]: St. Petersburg,St. Petersburg State University, 277 p. [In Russian.].

Kuptsova, A.V., Khudoley, A.K., Davis, W., Rainbird, R.H., and Molchanov, A.V., 2015, Results of the U-Pb age of detrital zircons from Upper Proterozoic deposits of the eastern slope of the Anabar uplift: Stratigraphy and Geological Correlation, v. 23, p. 246–261. doi:10.1134/S0869593815030053

Kuptsova, A.V., Khudoley, A.K., and Molchanov, A.V., 2011, Lithogeochemistry of Meso- and Neoproterozoic terrigenous rocks of the southeast Anabar Basin: Evolution of the composition of source rocks and epigenetic alterations, Vestnik St, Petersburg University, series 7, v. 1, p. 17–31. [In Russian.]

Kuz'min, V.K., Proskurnin, V.F., and Larionov, A.N., 2007, About the Late Riphean dating of the Snezhinsky complex granitoids (the north-east Taimyr) according to the zirconometry data: Zapiski of Russian Mineralogical Society (RMO), v. 136, no. 1, p. 42–49.

Kuznetsov, N., Belousova, E., Alekseev, A., and Romanyuk, T., 2014, New data on detrital zircons from the sandstones of the lower Cambrian Brusov Formation (White Sea region, East-European Craton): Unravelling the timing of the onset of the Arctida–Baltica collision: International Geology Review, v. 56, p. 1–19.

Kuznetsov, N.B., Natapov, L.M., Belousova, E.A., O`Reilly, S.Y., and Griffin, W.L., 2010, Geochronological,geochemical and isotopic study of detrital zircon suites from late Neoproterozoic clastic strata along the NE margin of the East European Craton: Implications for plate tectonic models: Gondwana Research, v. 17, p. 583–601. doi:10.1016/j.gr.2009.08.005

Li, Z.X., Bogdanova, S.V., Collins, A.S., Davidson, A., De Waele, B., Ernst, R.E., Fitzsimons, I.C.W., Fuck, R.A., Gladkochub, D.P., Jacobs, J., Karlstrom, K.E., Lu, S., Natapov, L.M., Pease, V., Pisarevsky, S.A., Thrane, K., and Vernikovsky, V., 2008, Assembly, configuration, and break-up history of Rodinia: A synthesis: Precambrian Research, v. 160, p. 179–210. doi:10.1016/j.precamres.2007.04.021

Li, Z.-X., Evans, D.A.D., and Halverson, G.P., 2013, Neoproterozoic glaciations in a revised global palaeogeography from the breakup of Rodinia to the assembly of Gondwanaland: Sedimentary Geology, v. 294, p. 219–232. doi:10.1016/j.sedgeo.2013.05.016

Linnemann, U., Gerdes, A., Drost, K., and Buschmann, B., 2007, The continuum between Cadomian orogenesis and opening of the Rheic Ocean: Constraints from LA-ICP-MS U-Pb zircon dating and analysis of plate-tectonic setting (Saxo-Thuringian zone, northeastern Bohemian Massif, Germany): Geological Society of America Special Papers, v. 423, p. 61–96.

Linnemann, U., Gerdes, A., Hofmann, M., and Marko, L., 2014, The Cadomian Orogen: Neoproterozoic to Early Cambrian crustal growth and orogenic zoning along the periphery of the West African Craton-Constraints from U-Pb zircon ages and Hf isotopes (Schwarzburg Antiform, Germany): Precambrian Research, v. 244, p. 236–278. doi:10.1016/j.precamres.2013.08.007

Lorenz, H., Gee, D.G., and Simonetti, A., 2008, Detrital zircon ages and provenance of the Late Neoproterozoic and Palaeozoic successions on Severnaya Zemlya, Kara Shelf: A tie to Baltica: Norwegian Journal of Geology, v. 88, p. 235–258.

Makariev, A.A., and Makarieva, E.M., 2012, Geological map T-45-48 of Russian Federation, cape chelyuskin: St. Petersburg, VSEGEI. Scale Scale 1:1 000 000, 1 sheet. [In Russian.]

Makhlaev, L.V., 1988, Tectonic nature of the Mamont-Shrenk terrane (Central Taimyr)/Doklady Akademii Nauk, Earth Sciences, v. 4, p. 77-87. [In Russian].

Markovsky, V.A., Schneider, O.V., Proskurnin, V.F., Kaban'kov, V.Y., Sobolevskaya, R.F., and Lopatin, B.G., 2003, Geological map T-45-47 of Russian Federation, Taimyr series: St. Petersburg, VSEGEI. scale 1: 1 000 000, 1 sheet. [In Russian.]

Melnikov, N.V., Yakshin, M.S., Shishkin, B.B., Efimov, A.O., Karlova, G.A., Kilkina, L.I., Konstantinova, L.N., Kochnev, B. B., Kraevskiy, B.G., Melnikov, P.N., Nagovitsin, K.E., Postnikov, A.A., Ryabkova, L.V., Terleev, A.A., and Khabarov, E.M., 2005, Stratigraphy of oil and gas basins of Siberia. Riphean and vendian of Siberian platform and its plaited border: Novosibirsk, Geo, 428 p. [In Russian.]

Metelkin, D.V., Vernikovsky, V.A., and Kazansky, A.Y., 2012, Tectonic evolution of the Siberian paleocontinent from the Neoproterozoic to the Late Mesozoic: Paleomagnetic record and reconstructions: Russian Geology and Geophysics, v. 39, p. 791–794.

Metelkin, D.V., Vernikovsky, V.A., and Matushkin, N.Y., 2015, Arctida between rodinia and pangea: precambrian research, v. 259, p. 114-129. doi:10.1016/j.precamres.2014.09.013

Miller, E.L., Kuznetsov, N., Soboleva, A., Udoratina, O., Grove, M. J., and Gehrels, G., 2011, Baltica in the Cordillera?: Geology, v. 39, p. 791–794. doi:10.1130/G31910.1

Pavlov, V.E., Gallet, Y., and Shatsillo, A.V., 2000, Paleomagnetism of the upper riphean lakhandinskaya group in the uchuro-maiskii area and the hypothesis of the late proterozoic supercontinent: Izvestiya Physics of Solid Earth, v. 36, no. 8, p. 638–648.

Pavlov, V.E., Shatsillo, A.V., Petrov, P.Y., 2015, Paleomagnetism of the upper Riphean deposits in the Turukhansk and Olenek uplifts and Uda Pre-Sayan region and the Neoproterozoic drift of the Siberian Platform: Izvestiya, Physics of the Solid Earth, v. 51, p. 716-747.

Payne, J.L., McInerney, D.J., Barovich, K.M., Kirkland, C.L., Pearson, N.J., and Hand, M., 2016, Strengths and limitations of zircon Lu-Hf and O isotopes in modelling crustal growth: Lithos, v. 248–251, p. 175–192. doi:10.1016/j.lithos.2015.12.015

Pease, V., Dovzhikova, E., Beliakova, L., and Gee, D.G., 2004, Late Neoproterozoic granitoid magmatism in the basement to the Pechora Basin, NW Russia: Geochemical constraints indicate westward subduction beneath NE Baltica: Geological Society, London, Memoirs, v. 30, p. 75–85. doi:10.1144/GSL.MEM.2004.030.01.08

Pease, V., Gee, D., Vernikovsky, V., Vernikovskaya, A., and Kireev, S., 2001, Geochronological evidence for late Grenvillian magmatic and metamorphic events in central Taimyr, northern Siberia: Terra Nova, v. 13, p. 270–280. doi:10.1046/j.1365-3121.2001.00351.x

Pease, V., and Scott, R., 2009, Crustal affinities in the Arctic Uralides, northern Russia: Significance of detrital zircon ages from Neoproterozoic and Palaeozoic sediments in Novaya Zemlya and Taimyr: Journal of the Geological Society, v. 166, p. 517–527. doi:10.1144/0016-76492008-093

Pease, V., 2011, Eurasian orogens and arctic tectonics: An overview, *in* Spencer, A.M., Embry, A.F., Gautier, P.L., Stoupakova, A.

V., and Soerensen, K., eds., Arctic petroleum geology: Geological Society, London, Memoirs, v. 35, p. 311–324.
Pease, V., and Vernikovsky, V., 2000, The tectono-magmatic evolution of the Taimyr Peninsula: Further constraints from new ion-microprobe data: Polarforschung, v. 68, p. 171–178.
Pisarevsky, S., Natapov, L.M., Donskaya, T.V., Gladkochub, D.P., Vernikovsky, V.A., Pisarevsky, S., Natapov, L.M., Donskaya, T.V., Gladkochub, D.P., and Vernikovsky, V.A., 2008, Proterozoic Siberia: A promontory of Rodinia: Precambrian Research, v. 160, p. 66–76. doi:10.1016/j.precamres.2007.04.016
Pisarevsky, S.A., Gladkochub, D.P., Konstantinov, K.M., Mazukabzov, A.M., Stanevich, A.M., Murphy, J.B., Tait, J.A., Donskaya, T.V., and Konstantinov, I.K., 2013, Paleomagnetism of Cryogenian Kitoi mafic dykes in South Siberia: Implications for Neoproterozoic paleogeography: Precambrian Research, v. 231, p. 372–382. doi:10.1016/j.precamres.2013.04.007
Pogrebitsky, Y.E., and Shanurenko, N.K., 1998, Explanatory note to Geological Map S-47-49 of Russian Federation (Lake Taimyr): St. Petersburg, VSEGEI, 231 p. [In Russian.]
Popov, V.Y., Berezyuk, N.I., and Paderin, P.G., Geological Map T-48-XXXI, XXXII, XXXIII of the Russian Federation. Taimir series: Scale 1: 200 000, 1 sheet. (unpublished).
Priyatkina, N., Khudoley, A.K., Collins, W.J., Kuznetsov, N.B., and Huang, H.-Q., 2016, Detrital zircon record of Meso- and Neoproterozoic sedimentary basins in northern part of the Siberian Craton: Characterizing buried crust of the basement: Precambrian Research, v. 285, p. 21–38. doi:10.1016/j.precamres.2016.09.003
Prokopiev, A.V., Khudoley, A.K., Koroleva, O.V., Kazakova, G.G., Lokhov, D.K., Malyshev, S.V., Zaitsev, A.I., Roev, S.P., Sergeev, S.A., Berezhnaya, N.G., and Vasiliev, D.A., 2016, The Early Cambrian bimodal magmatism in the northeastern Siberian Craton: Russian Geology and Geophysics, v. 57, p. 155–175. doi:10.1016/j.rgg.2016.01.011
Proskurnin, V.F., ed., 2009, Explanatory note to geological map S-48 of the Russian Federation (Lake Taimyr): St. Petersburg, VSEGEI, 253 p. scale 1: 1 000 000. [In Russian.]
Proskurnin, V.F., Gavrish, A.V., Tarnogradsky, V.D., Bagaeva, A. A., Mezhubovsky, V.V., and Trofimov, V.V., 2009, Geological map S-48 of the Russian Federation (Lake Taimyr): St. Petersburg, VSEGEI. scale 1: 1 000 000, 1 sheet. [In Russian.]
Proskurnin, V.F., Schneider, G.V., Bagaeva, A.A., and Borisenkov, K.V., 2016, Geological map S-48-I, II of Russian Federation: St. Petersburg, VSEGEI. Scale 1:200 000, 1 sheet (aauthor's personal copy accepted to publication). [In Russian.]
Proskurnin, V.F., Vernikovsky, V.A., Metelkin, D.V., Petrushkov, B.S., Vernikovskaya, A.E., Gavrish, A.V., Bagaeva, A.A., Matushkin, N.Y., Vinogradova, N.P., and Larionov, A.N., 2014, Rhyolite–granite association in the Central Taimyr zone: Evidence of accretionary-collisional events in the Neoproterozoic: Russian Geology and Geophysics, v. 55, p. 18–32. doi:10.1016/j.rgg.2013.12.002
Rainbird, R.H., Stern, R.A., Khudoley, A.K., Kropachev, A.P., Heaman, L.M., and Sukhorukov, V.I., 1998, U–Pb geochronology of Riphean sandstone and gabbro from southeast Siberia and its bearing on the Laurentia–Siberia connection: Earth and Planetary Science Letters, v. 164, p. 409–420. doi:10.1016/S0012-821X(98)00222-2
Roberts, D., and Siedlecka, A., 2002, Timanian orogenic deformation along the northeastern margin of Baltica, northwest Russia and northeast Norway, and Avalonian– Cadomian connections: Tectonophysics, v. 352, p. 169–184. doi:10.1016/S0040-1951(02)00195-6
Romanyuk, T.V., Kuznetsov, N.B., Maslov, A.V., Belousova, E.A., Krupenin, M.T., Ronkin, Y.L., Gorozhanin, V.M., and Gorozhanina, E.N., 2014, Geochemical and Lu/Hf isotopic (LA-ICP-MS) signature of detrital zircons from sandstones of the basal levels of the Riphean stratotype: Doklady Earth Sciences, v. 459, p. 1356–1360. doi:10.1134/S1028334X14110257
Rosen, O.M., 2003, The Siberian craton: Tectonic zonation and stages of evolution: Geotectonics, v. 37, p. 175–192.
Rosen, O.M., Condie, K., Natapov, L.M., and Nozhkin, A.D., 1994, Archean and Early Precambrian evolution of the Siberian craton: A preliminary assessment, *in* Condie, K.C., eds., Archean crustal evolution: Amsterdam, Elsevier, p. 411–459.
Scotese, C.R., 2013, PALEOMAP Project. http://www.scotese.com. (December 2013).
Sears, J.W., 2012, Transforming Siberia along the Laurussian margin: Geology, v. 40, p. 535–538. doi:10.1130/G32952.1
Sears, J.W., and Price, R.A., 2000, New look at the Siberian connection: No SWEAT: Geology, v. 28, p. 423–426. doi:10.1130/0091-7613(2000)28<423:NLATSC>2.0.CO;2
Semikhatov, M.A., and Serebryakov, S.N., 1983, Siberian hypostratotype of riphean: Nauka, Moscow, 223 p. [In Russian.]
Shatsillo, A., Pavlov, V., and Didenko, A., 2006, Paleomagnetism of Vendian rocks in the southwest of the Siberian Platform: Russian Journal of Earth Sciences, no. 8, p. 1–30. doi:10.2205/2005ES000182
Shi, Y., Yu, J.-H., and Santosh, M., 2013, Tectonic evolution of the Qinling orogenic belt, Central China: New evidence from geochemical, zircon U–Pb geochronology and Hf isotopes: Precambrian Research, v. 231, p. 19–60. doi:10.1016/j.precamres.2013.03.001
Smethurst, M.A., Khramov, A.N., and Torsvik, T.H., 1998, The Neoproterozoic and Palaeozoic palaeomagnetic data for the Siberian Platform: From Rodinia to Pangea: Earth-Science Reviews, v. 43, p. 1–24. doi:10.1016/S0012-8252(97)00019-6
Smits, R.G., Collins, W.J., Hand, M., Dutch, R., and Payne, J., 2014, A Proterozoic Wilson cycle identified by Hf isotopes in central Australia: Implications for the assembly of Proterozoic Australia and Rodinia: Geology, v. 42, p. 231–234. doi:10.1130/G35112.1
Sovetov, J.K., Kulikova, A.E., and Medvedev, M.N., 2007, Sedimentary basins in the southwestern Siberian craton: Late Neoproterozoic–Early Cambrian rifting and collisional events: Geological Society of America Special Papers, v. 423, p. 549–578.
Uflyand, A.K., Natapov, L.M., Lopatin, V.M., and Chernov, D.V., 1991, To the Taimyr tectonic nature: Geotectonics, v. 6, p. 76–93. [In Russian.]
Vernikovsky, V.A., 1995, Riphean and Paleozoic metamorphic complexes of the Taymyr Foldbelt: Conditions of formation: Petrology, v. 3, p. 55–72. [In Russian.]
Vernikovsky, V.A., 1996, Geodynamic evolution of Taimyr fold area: Novosibirsk, SPC UIGGM SB RAS, 203 p. [In Russian.]
Vernikovsky, V.A., Dobretsov, N.L., Metelkin, D.V., Matushkin, N. Y., and Koulakov, I.Y., 2013, Concerning tectonics and the tectonic evolution of the Arctic: Russian Geology and Geophysics, v. 54, p. 838–858. doi:10.1016/j.rgg.2013.07.006
Vernikovsky, V.A., Kotov, A.B., Ponomarchuk, V.A., Sal'nikova, E. B., Kovach, V.P., and Travin, A.V., 1997, Late Riphean–Vendian history in Taimyr: Sm–Nd, Rb–Sr, K–Ar age of

garnet amphibolites of the Stanovoy ophiolite belt: Dokalady Earth Sciences, v. 352, p. 218–221. [In Russian.]

Vernikovsky, V.A., Metelkin, D.V., Vernikovskaya, A.E., Sal'nikova, E.B., Kovach, V.P., and Kotov, A.B., 2011, The oldest island arc complex of Taimyr: Concerning the issue of the Central-Taimyr accretionary belt formation and paleogeodynamic reconstructions in the arctic: Doklady Earth Sciences, v. 436, p. 186–192. doi:10.1134/S1028334X1102019X

Vernikovsky, V.A., Sal'nikova, E.B., Kotov, A.B., Kovach, V.P., and Yakovleva, S.Z., 1998, Precambrian granites of the Faddey terrane: New geochemical and geochronologic (U–Pb, Sm–Nd) data: Doklady Russian Academy of Sciences (RAN), v. 363, no. 5, p. 653–657. [In Russian.]

Vernikovsky, V.A., Vernikovskaya, A.E., Chernykh, A.I., and Melgunov, M.S., 1996, Petrology and geochemistry of Taimyr Riphean ophiolites: Russian Geology and Geophysics, v. 36, p. 103–120. [In Russian.]

Vernikovsky, V.A., Vernikovskaya, A.E., Lyapunov, S.M., Neimark, L.A., Proskurnin, V.F., Chernykh, A.I., and Safonova, I.Y., 1994, Petrology,geochemistry, and tectonic settings of plagiogranites of the Chelyuskin Ophiolite Belt: International Geology Review, v. 36, p. 961–974. doi:10.1080/00206819409465498

Vernikovsky, V.A., Vernikovskaya, A.E., Pease, V.L., and Gee, D. G., 2004, Neoproterozoic Orogeny along the margins of Siberia: London: Geological Society, Memoirs, v. 30, p. 233–248. doi:10.1144/GSL.MEM.2004.030.01.18

Vernikovsky, V.A., and Zabiyaka, A.I., 1985, Metamorphic complexes of the Northern-Eastern Taimyr: Soviet Geology and Geophysicss, v. 26, p. 50–57. [In Russian.]

Wang, H., Wu, Y.-B., Gao, S., Qin, Z.-W., Hu, Z.-C., Zheng, J.-P., and Yang, S.-H., 2016a, Continental growth through accreted oceanic arc: Zircon Hf-O isotope evidence for granitoids from the Qinling orogeny: Geochimica Et Cosmochimica Acta, v. 182, p. 109–130. doi:10.1016/j.gca.2016.03.016

Wang, Z.-W., Pei, F.-P., Xu, W.-L., Cao, -H.-H., Wang, Z.-J., and Zhang, Y., 2016b, Tectonic evolution of the eastern Central Asian Orogenic Belt: Evidence from zircon U–Pb–Hf isotopes and geochemistry of early Paleozoic rocks in Yanbian region, NE China: Gondwana Research, v. 38, p. 334–350. doi:10.1016/j.gr.2016.01.004

Watt, G., Kinny, P., and Friderichsen, J., 2000, U–Pb geochronology of Neoproterozoic and Caledonian tectonothermal events in the East Greenland Caledonides: Journal of the Geological Society, v. 157, p. 1031–1048. doi:10.1144/jgs.157.5.1031

Winchester, J., and Floyd, P., 1977, Geochemical discrimination of different magma series and their differentiation products using immobile elements: Chemical Geology, v. 20, p. 325–343. doi:10.1016/0009-2541(77)90057-2

Wood, D.A., 1980, The application of a Th-Hf-Ta diagram to problems of tectonomagmatic classification and to establishing the nature of crustal contamination of basaltic lavas of the British Tertiary Volcanic Province: Earth and Planetary Science Letters, v. 50, p. 11–30. doi:10.1016/0012-821X(80)90116-8

Yang, J.-H., Wu, F.-Y., Wilde, S., Xie, L.-W., Yang, Y.-H., and Liu, X.-M., 2006, Tracing magma mixing in granite genesis: In situ U–Pb dating and Hf-isotope analysis of zircons: Contributions to Mineralogy and Petrology, v. 153, p. 177–190. doi:10.1007/s00410-006-0139-7

Zonenshain, L.P., Kuzmin, M.I., and Natapov, L.M., 1990, Geology of the USSR: A plate tectonic synthesis: American Geophysical Union: Geodynamics Series, v. 21, p. 242 p.